



OPEN ACCESS

ORIGINAL ARTICLE

Genome-wide DNA methylation analysis of patients with imprinting disorders identifies differentially methylated regions associated with novel candidate imprinted genes

Louise E Docherty,^{1,2} Faisal I Rezwan,¹ Rebecca L Poole,^{1,2} Hannah Jagoe,¹ Hannah Lake,¹ Gabrielle A Lockett,¹ Hasan Arshad,^{1,3} David I Wilson,¹ John W Holloway,¹ I Karen Temple,^{1,4} Deborah J G Mackay^{1,2}

► Additional material is published online only. To view please visit the journal online (<http://dx.doi.org/10.1136/jmedgenet-2013-102116>).

¹Faculty of Medicine, University of Southampton, Southampton, UK

²Wessex Regional Genetics Laboratory, Salisbury NHS Foundation Trust, Salisbury, UK

³David Hyde allergy centre Isle of Wight, UK

⁴Wessex Clinical Genetics Service, Princess Anne Hospital, University Hospital Southampton NHS Foundation Trust, Southampton, UK

Correspondence to

Dr D J G Mackay, Wessex Regional Genetics Laboratory, Salisbury District Hospital, Salisbury SP2 8BJ, UK; djgm@soton.ac.uk

LED and FIR contributed equally to this study.

Received 14 October 2013

Revised 4 November 2013

Accepted 9 December 2013

Published Online First

5 February 2014



Open Access
Scan to access more
free content

To cite: Docherty LE, Rezwan FI, Poole RL, et al. *J Med Genet* Published Online First: [please include Day Month Year] doi:10.1136/jmedgenet-2013-102116

ABSTRACT

Background Genomic imprinting is allelic restriction of gene expression potential depending on parent of origin, maintained by epigenetic mechanisms including parent of origin-specific DNA methylation. Among approximately 70 known imprinted genes are some causing disorders affecting growth, metabolism and cancer predisposition. Some imprinting disorder patients have hypomethylation of several imprinted loci (HIL) throughout the genome and may have atypically severe clinical features. Here we used array analysis in HIL patients to define patterns of aberrant methylation throughout the genome.

Design We developed a novel informatic pipeline capable of small sample number analysis, and profiled 10 HIL patients with two clinical presentations (Beckwith–Wiedemann syndrome and neonatal diabetes) using the Illumina Infinium Human Methylation450 BeadChip array to identify candidate imprinted regions. We used robust statistical criteria to quantify DNA methylation.

Results We detected hypomethylation at known imprinted loci, and 25 further candidate imprinted regions (nine shared between patient groups) including one in the Down syndrome critical region (*WRB*) and another previously associated with bipolar disorder (*PPIEL*). Targeted analysis of three candidate regions (*NHP2L1*, *WRB* and *PPIEL*) showed allelic expression, methylation patterns consistent with allelic maternal methylation and frequent hypomethylation among an additional cohort of HIL patients, including six with Silver–Russell syndrome presentations and one with pseudohypoparathyroidism 1B.

Conclusions This study identified novel candidate imprinted genes, revealed remarkable epigenetic convergence among clinically divergent patients, and highlights the potential of epigenomic profiling to expand our understanding of the normal methylome and its disruption in human disease.

INTRODUCTION

Genomic imprinting is the epigenetic regulation of gene expression by parent of origin. DNA methylation at imprinting control regions (ICRs) is the most robust and widely studied epigenetic modification regulating imprinting. Genomic imprinting requires resetting of DNA methylation in the

germline and its subsequent resistance to erasure during the transition from germ cell to early embryonic development.^{1–2} While methylation at ICRs is ubiquitous and permanent, the effects on DNA methylation and expression of surrounding genes are dependent on other factors such as tissue and developmental stage.³

Many imprinted loci were identified through the developmental disorders caused by their disruption, and particularly the discovery of uniparental disomy and other genetic errors in rare human disorders of imprinting.^{4–5} But the total number of imprinted genes is not known. Recent efforts to identify imprinted genes by murine transcriptome analysis yielded high numbers of transcripts with allelic bias.⁶ However, this observation has been disputed and may be attributable to various technical sources of skewed allelic representation in RNA-seq data⁷ and, more recently, genome-wide bisulfite sequencing has allowed direct assessment of allele-specific methylation;⁸ taken together, these observations suggest that our current catalogue of imprinted genes is approaching completion, with few novel germline imprints remaining to be discovered (<http://igc.otago.ac.nz>).⁹

Many known imprinted genes are regulators of growth and development, and their expression at critical developmental times is functionally hemizygous. Therefore, alteration of effective copy number can cause developmental disorders.¹⁰ To date, eight imprinting disorders (IDs) have been identified: Beckwith–Wiedemann syndrome (BWS; MIM #130659), Silver–Russell syndrome (SRS; MIM #180860), transient neonatal diabetes (TND) mellitus (MIM #601410), Prader–Willi syndrome (MIM #176270), Angelman syndrome (MIM #105830), matUPD14-like (Temple syndrome) and patUPD14-like syndromes, and pseudohypoparathyroidism 1B (PHP-1B; MIM #103580). Aetiological mechanisms of IDs include UPD, copy number variation, mutation of the expressed copy, or epimutation secondary to or independent of a predisposing genetic mutation. A subset of patients with IDs have epimutations affecting multiple imprinted loci across the genome (multi-locus methylation disorders or hypomethylation of imprinted loci (HIL)¹¹). The reported rate of HIL in BWS is 38% (with ICR2

hypomethylation), 57% in TND (with *PLAGL1* hypomethylation) and 10% in SRS (with *ICR1* hypomethylation).^{12–14} There is no standard quantification for hypomethylation at the affected loci, though tissue mosaicism is thought to account for the variation observed between patients. In some of these disorders, a shared pattern of methylation derangement can be detected, and underlying genetic mutations have been identified;^{15–18} in other cases, the cause(s) remain unknown.

In order to identify novel imprinted regions, several groups have used genome-wide methylation analyses of patients with UPD and HIL, commonly using the Infinium Human Methylation27 BeadChip array.^{19–21} The potential limitations of this approach include the limited coverage of this array, and the lack of suitable bioinformatic pipelines to study large methylation changes in small study cohorts, as currently available pipelines are designed to assess modest DNA methylation changes in large study cohorts.^{22–24} To address these limitations, we used the Infinium Human Methylation450 BeadChip array, and developed a new analysis pipeline capable of robust analysis of small study groups with large methylation changes.

Here, we analysed the methylomes of 10 HIL patients with two clinical presentations (five BWS and five neonatal diabetes), compared with normal controls, and identified hypomethylated regions, including three hitherto undescribed candidate imprinted regions.

MATERIALS AND METHODS

Study population (ethics)

Peripheral blood leucocyte DNA of patients with IDs was assessed by methylation-specific PCR (msPCR) at 11 maternally methylated loci, as described (see online supplementary table S1; the majority of these patients have been previously reported in Poole *et al*¹²). Those patients with hypomethylation at loci additional to the primary locus for their presenting disorder were classified as HIL, and subgrouped using the epigenetic profiles of these 11 maternal imprinted loci. It was apparent that five patients with TND and five with BWS showed an overlapping pattern of hypomethylation: TND-HIL samples showed hypomethylation at *PLAGL1*, *DIRAS*, *IGF2R* and *IGF1R* differentially methylated regions (DMRs), with some additional overlap of hypomethylation at *MEST*, *KCNQ1OT1* and *GRB10*, and BWS-HIL patients shared hypomethylation of *KCNQ1OT1*, *PLAGL1*, *IGF2R* and *MEST*, with *NESPAS* and *GNAS* hypomethylation observed in 2/5 patients. These patients were selected for further analysis to determine whether they had additional shared hypomethylation patterns.

All TND-HIL patients were negative for *ZFP57* mutations and BWS-HIL patients negative for *NLRP2* mutations. The ethical approval for the use of these samples was obtained through the study 'Imprinting Disorders Finding Out Why?', approved by Southampton and South West Hampshire Research Ethics committee 07/H0502/85 and 'Mapping clinical and molecular studies of 6q24 transient neonatal diabetes' approved by Wiltshire Research Ethics committee 08/H0104/15.

Control population

Control group 1 (N=221) and control group 2 (N=245) anonymous batch-matched healthy samples from an unrelated study were used to generate control methylation profiles for the analysis of TND-HIL and BWS-HIL cases, respectively. Control group 1 samples were mixed gender and source material, with 198 peripheral blood leucocytes DNA samples derived from cohort members and their partners and 23 cord blood leucocytes DNA samples from their offspring whereas control group

2 contained 221 peripheral blood leucocyte DNA samples from female subjects at 18 years of age from an unselected population birth cohort. Ethical approval was obtained from the Isle of Wight Local Research Ethics Committee (now named the National Research Ethics Service, NRES Committee South Central—Southampton B) for the 18 years follow-up (06/Q1701/34) and NRES Committee South Central—Hampshire B (09/H0504/129) for the third generation study.

Validation samples

Methylation array findings were validated by targeted testing of DNA and RNA samples. DNA was derived from two hydatidiform mole cell lines, peripheral blood leucocytes of 92 anonymised controls, four anonymised normal trios and 34 anonymised individuals diagnosed with Down syndrome, and patients with IDs: five TND-HIL, six BWS-HIL, seven SRS-HIL, one PHP-HIL, five *ZFP57* mutation cases presenting with TND and nine patients with hypomethylation at only one locus (two TND with *PLAGL1* hypomethylation, two BWS patients with *KCNQ1OT1* hypomethylation, four SRS patients with *ICR1* hypomethylation and one with UPD7mat). These samples were obtained under the same ethical approval as the study group and previously reported.¹² Nucleic acids (DNA and RNA) from human embryonic and fetal tissues were obtained with informed consent and with permission from the Southampton and South West Hampshire joint Research Ethics Committee, staged according to the Carnegie classification or foot length.

Array-based methylation analysis

1250 ng of Qubit 2.0 Fluorometer quantified DNA was bisulfite-treated using the EZ 96-DNA methylation kit (Zymo Research, California, USA), following the manufacturer's standard protocol. Genome-wide DNA methylation was assessed by The Oxford Genomics Centre using the Illumina Infinium HumanMethylation450 BeadChip (Illumina, Inc., California, USA). Arrays were processed using the manufacturer's standard protocol with multiple identical control samples assigned to each bisulfite conversion batch to assess assay variability and samples randomly distributed on microarrays to control against batch effects. The BeadChips were scanned using a BeadStation, and the methylation level (β value) calculated for each queried CpG locus using the Methylation Module of BeadStudio software.

Data preprocessing and quality control

A pipeline was developed using the Illumina methylation analysis (IMA) package within the R statistical analysis environment (<http://www.r-project.org>).²² Data from five TND-HIL and five BWS-HIL samples were grouped and run in this pipeline independently. Sites were removed that contain any missing values. All samples met minimal inclusion criteria for analysis, as each sample had >75% sites with a detection p value $<1 \times 10^{-5}$. In all, 216 sites were removed from TND-HIL study and 106 from BWS-HIL study, as these had detected p value >0.05 in at least 75% of the sample analysed. Among these removed sites, 68 are common between the two study groups. Initial QC-plots (see online supplementary figure S1) for both of the studies showed that male and female samples clustered together via unsupervised clustering resulting from gender-specific biases in methylation level.^{23–24} Therefore, probes on X and Y chromosomes were removed to discard any sex bias within the samples. The number of sites annotated by probe types that were removed by the initial quality control step is shown in online supplementary table S2. A total of 76.88% probes remained for the TND-HIL

analysis and 81.82% remained for the BWS-HIL analysis after the preprocessing.

The β -values were converted to M-values by logit transformation as M-value increases the cogency of statistical tests for differential methylation.²⁵ Quantile normalisation was used to normalise signal intensities for each probe and reduce inter-array variation.²⁶

Illumina Human 450 K methylation array uses two different chemistries, Infinium I and II, to enhance the breadth of coverage. Infinium I uses two probes per CpG locus (both methylated and unmethylated query probes), whereas in Infinium II only one probe (either methylated or unmethylated) per CpG locus is required. To correct these differences in the results between these two chemistries, peak correction was applied.²⁷ No batch correction was required as all the cases and controls for individual experiments had been processed in the same batch.

Low sample number differential methylation analysis

Stringent criteria were set to select candidate imprinted sequences hypomethylated in patients, with p values adjusted using false discovery rate to ensure statistical robustness.²⁸ Individual CpGs were selected when hypomethylated in patients compared with controls, with an adjusted p value of $>1.33 \times 10^{-7}$, and an M-value between +1 and -1 (equivalent to $0.26 \leq \beta \leq 0.7$) in normal controls. Genes containing two CpGs meeting these criteria and within <2000 nucleotides were deemed to be candidate DMRs.

Initially paired t test and one-sample t test were used for statistical analysis; however, these methods did not reveal any probes meeting our stringent criteria, probably because of the low sample number. Therefore, we explored the linear model technique, used for analysis of microarray data,²⁹ which models the significant part of the data and then allows the fitted coefficients to be compared in as many ways as possible. Crawford and Garthwaite proved that using a larger control group can produce significant statistical results even for a single case provided that appropriate statistical methods are applied.³⁰ Therefore, for both of the case groups, we used larger numbers of controls ($n > 200$) against smaller numbers of cases ($n = 5$). The linear model achieved convincing statistical outcomes from our pipeline, with efficient identification of known and novel hypomethylated loci for both TND-HIL and BWS-HIL case groups. Using the same criteria, only one region of hypermethylation was found in TND-HIL and four in BWS-HIL; these were not further examined as they were not relevant to this study (data not shown).

Targeted validation testing

msPCR analysis of the 11 maternally methylated loci used previously described primers and protocols.¹² msPCR primers for candidate loci *NHP2L1*, *PPIEL* and *WRB* are listed in online supplementary table S3.

Bisulfite sequencing

Bisulfite-specific primers were designed to amplify regions of 80–180 nt containing 7–12 CpG dinucleotides, using PyroMark software V1.0 (Qiagen). Primer sequences are listed in online supplementary table S3. Amplicons were generated (Phusion DNA polymerase New England BioLabs) from two patients and two controls, ligated into pCR2.1 (Invitrogen); 2 μ L of each ligation was transformed into chemically competent TOP10 cells (Invitrogen). Positive clones were selected on agar plates supplemented with 40 μ g/mL X-gal and 100 μ g/mL ampicillin. Overall, 24 white colonies were selected from each plate and

suspended in 50 μ L dH₂O prior to denaturation (94°C for 5 min). An amount of 1 μ L of the denatured bacterial solution was used as a PCR template for M13 primer amplification (Phusion DNA polymerase New England BioLabs). These reactions were treated with ExoSAP to degrade remaining primers, prior to sequencing with M13 forward and reverse primers. Very similar results were obtained for the two controls and the two patients; results from only one patient and one control are presented in the figures.

Restriction digest sequencing

To determine whether methylation was allele-specific or restricted by parent of origin, SNPs were analysed in proximity to DMRs in DNA from family trios. Heterozygous SNPs were identified and their inheritance determined by Sanger sequencing in DNA of offspring and parents. To determine methylation status, 200 ng of offspring DNA was digested before amplification with restriction enzymes BstU1 or Mcrbc (New England Biolabs) according to manufacturer's instructions, as described.³¹

Expression analysis

Coding SNPs were identified within novel imprinting gene candidates *WRB* and *NHP2L1* (rs13230 and rs8779, respectively). These were used to identify heterozygous samples collected following termination of pregnancy for a non-medical/social reason at gestational age 8–12 weeks with RNA-matched samples for a range of tissues (primers listed in online supplementary table S3). Allele-specific expression was then assessed in available heterozygous embryonic tissues.

cDNA was prepared with SuperScript III reverse transcriptase (Invitrogen) from 500 ng embryonic RNA. RT-PCR primers were designed to detect different isoforms of the candidate genes (see online supplementary table S3) and were amplified using Phusion DNA polymerase (New England BioLabs).

RESULTS

Statistical analysis of 450 K methylation array data

We developed a new analysis pipeline to detect methylation changes, with stringent selection criteria, capable of robust analysis of our small epigenetically defined groups (see Materials and methods section). The pipeline employed the linear modelling commonly used for microarray analysis and compared small patient numbers against a large control group to produce significant statistical results.^{29–30} Using stringent selection criteria, 34 hypomethylated regions were identified in the BWS-HIL cohort and 21 regions in TND-HIL (figure 1, see online supplementary tables S4 and S5).

The hypomethylated regions generated from both groups included several known imprinted genes (table 1, see online supplementary tables S4 and S5), both within and outside the 11 loci previously assessed in targeted analysis. The p values observed for known loci were proportionate to the degree of hypomethylation predicted from msPCR analysis of the patients groups. This is most clearly demonstrated at the disease-specific loci, where the lowest adjusted p value for the TND locus *PLAGL1* was more significant in TND-HIL than BWS-HIL (4.84×10^{-124} vs 4.39×10^{-51}) (see online supplementary figure S2B, supplementary tables S4 and S5) and, conversely, the BWS locus *KCNQ1OT1* had a lower p value in BWS-HIL than TND-HIL cohort (4.27×10^{-68} vs 9.47×10^{-10}) (see online supplementary tables S4 and S5). These p values were consistent with the degree of hypomethylation detected by targeted testing (see online supplementary table S1).

To assess the effect of merging patient data on the ability of the pipeline to detect hypomethylation, we used *SNRPN*, the

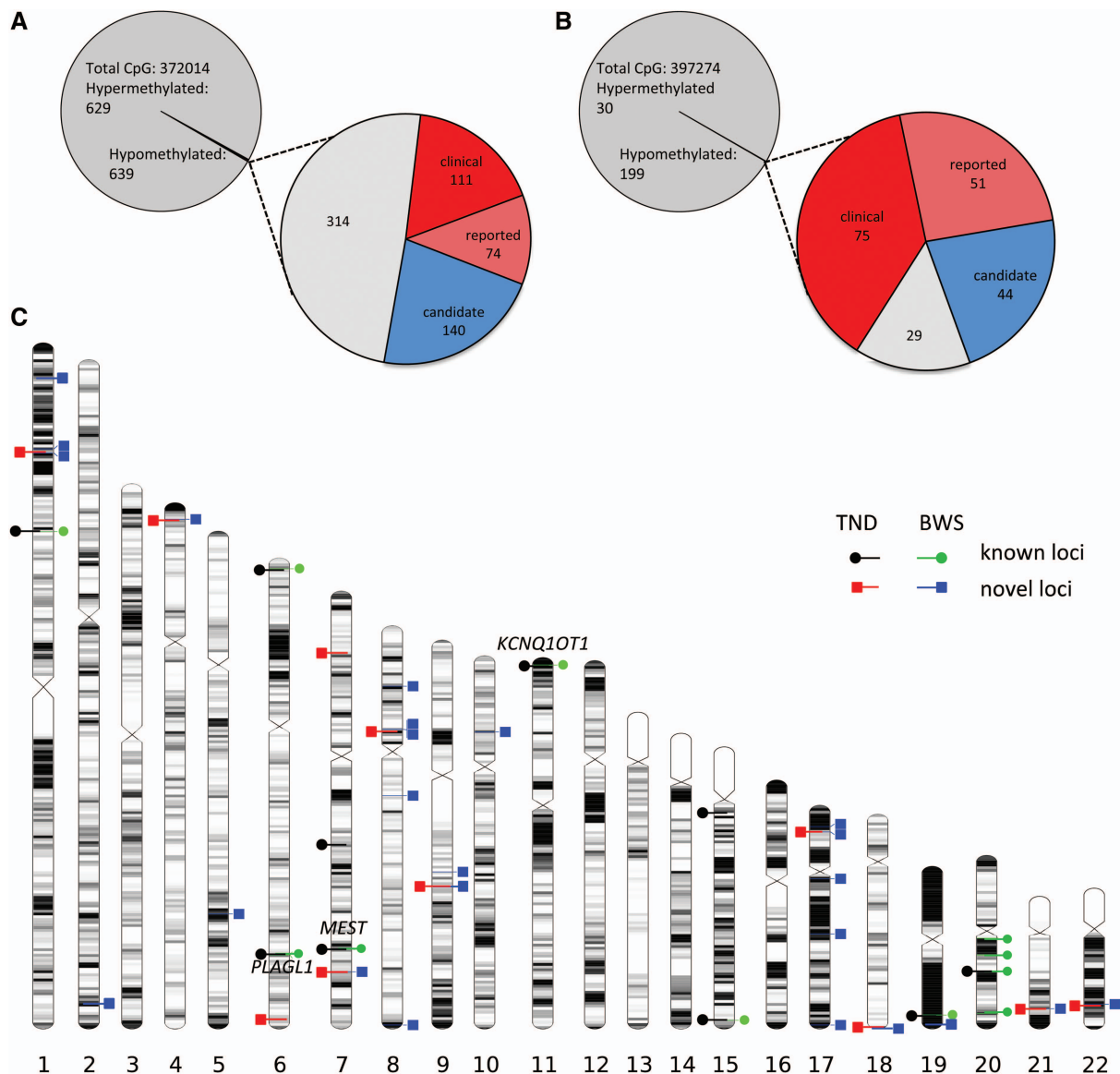


Figure 1 Distribution of known and candidate differentially methylated CpG sites in (A) Beckwith–Wiedemann syndrome (BWS) and (B) transient neonatal diabetes (TND). In each case, the pie chart to the left shows CpG sites compared between cases and controls (in grey), including those meeting criteria for differential methylation; the pie chart to the right highlights hypomethylated CpG sites, including those in known clinically-relevant loci (red), loci reported to be imprinted (pink) and loci not currently reported to be imprinted, that is, candidate loci (blue). (C) Chromosome ideogram showing the distribution across all autosomes of known and candidate differentially methylated loci. Black dots represent known imprinted genes that were shown to be hypomethylated in the TND patient group in this study; the green dots represent known imprinted genes shown to be hypomethylated in the BWS patient group in this study. Red and blue squares correspond to candidate imprinted loci in TND-HIL and BWS-HIL, respectively. The names of imprinted loci associated with imprinting disorders are displayed next to loci, in black, where they were detected as hypomethylated in patient samples.

only locus identified by msPCR in both patient groups with hypomethylation of a single patient (see online supplementary table S1). Using our criteria, hypomethylation of *SNRPN* was resolved in the TND-HIL, but not the BWS-HIL cohort where the hypomethylation was less severe (table 1, see online supplementary table S6). Thus, the pipeline was proved to resolve moderate hypomethylation in a single individual, validating the analysis of these hyper-rare patients as a group, rather than attempting analysis of single patients, which presents significant statistical challenges.

In addition to the known imprinted regions, 23 and 11 novel candidate DMRs were detected in the BWS-HIL and TND-HIL cohorts, respectively. Nine of these candidate DMRs were shared between BWS-HIL and TND-HIL patient groups (table 1). It is

noteworthy that the coverage of probes was broadly higher in known imprinted genes than novel candidates (eg, 54 in *PLAGL1*, 267 in *KCNQ1* and 73 in *MEST*, compared with 24 in *ERLIN2*, 28 in *WRB*, 23 in *NHP2L1* and 13 in *LOC728448*), reducing the likelihood of finding such novel candidates by chance.

Validation of differential methylation region candidates

Candidates were prioritised for follow-up based on prior evidence of allele-specific methylation in primary cell lines and hypomethylation in sperm (from Fang *et al*³²) which would be consistent with maternal imprinting (this eliminated *JAKMIP1* and *GLP2R*). Further inspection highlighted three candidates (*NHP2L1*, *WRB* and *PPIEL*) where hypomethylation affected sequence contexts characteristic of imprinted genes (figures 2

Table 1 Hypomethylated regions shared between TND-HIL and BWS-HIL patients

Candidate	Chr	Gene name	CpG island	BWS			TND		
				Probe region*	No. probes†	Lowest p value‡	Probe region*	No. probes†	Lowest p value‡
Novel candidate DMRs	1	LOC728448/ <i>PP1EL</i>	No	40 024 971–40 025 411	3	1.47E–18	40 024 971–40 025 232	2	3.09E–22
	4	JAKMIP1	Yes	6 107 021–6 107 339	4	2.48E–16	6 107 021–6 107 339	4	5.83E–36
	7	SVOP1	Yes	138 348 774–138 349 443	3	6.30E–41	138 348 774–138 349 443	3	7.21E–20
	9	FANCC	Yes	98 075 481–98 075 492	2	8.29E–58	98 075 481–98 075 492	2	7.28E–55
	17	GLP2R	No	9 729 250–9 729 424	3	3.33E–16	9 729 250–9 729 422	4	1.81E–23
	21	<i>WRB</i>	Yes	40 757 691–40 758 208	2	2.51E–20	40 757 691–40 758 208	4	6.71E–29
	8	LOC728024/ <i>ERLIN2</i>	No	37 605 517–37 605 783	4	3.87E–40	37 605 359–37 605 978	6	2.69E–42
	18	LOC100130522/ <i>PARD6G-AS1</i>	Yes	77 905 355–77 905 947	3	1.01E–19	77 905 298–77 905 947	9	4.38E–71
Imprinted—not associated with ID	22	<i>NHP2L1</i>	Yes	42 078 217–42 078 723	6	4.08E–15	42 078 217–42 078 723	6	4.25E–54
	1	<i>DIRAS3</i> ⁴³	Yes	68 512 539–68 517 273	21	6.69E–31	68 512 539–68 517 273	20	5.45E–64
	6	<i>FAM50B</i> ^{20 44}	Yes	3 849 235–3 849 818	17	1.70E–18	3 849 272–3 849 818	17	1.64E–39
	15	<i>IGF1R</i> ⁴⁵	No	99 408 636–99 409 506	5	2.23E–15	99 408 636–99 409 957	6	1.04E–36
	19	<i>ZNF331</i> ^{46 47}	Yes	54 040 774–54 058 085	11	1.39E–40	54 040 813–54 058 085	10	9.13E–53
Imprinted—associated with ID	20	<i>L3MBTL</i> ⁴⁸	Yes	42 142 417–42 143 502	13	1.32E–17	42 142 417–42 143 489	18	7.60E–25
	6	<i>PLAGL1</i>	Yes	144 328 421–144 329 909	14	1.06E–55	144 328 482–144 329 909	15	1.22E–129
	7	<i>MEST</i>	Yes	130 130 187–130 133 110	42	6.12E–42	130 130 383–130 133 110	42	1.73E–45
	11	<i>KCNQ1</i>	Yes	2 715 837–2 722 258	26	1.14E–73	2 720 463–2 722 119	9	4.86E–13

Datasets from five patients with BWS-HIL and five with TND-HIL were compared with datasets from 245 and 211 batch-matched normal controls, respectively. Probes with M-values between –1 and +1 in controls and relative hypomethylation in patients with a p value of <1.33E–7 were identified. This subset was further filtered by minimal criteria for a hypomethylated locus, that is, ≥2 hypomethylated probes spaced by <2000 nucleotides. Candidate regions that meet these criteria in both BWS-HIL and TND-HIL are listed in this table.

*Genome position of most proximal and distal probe fulfilling hypomethylation criteria.

†Number of probes within the locus fulfilling hypomethylation criteria.

‡Minimum p value among probes fulfilling hypomethylation criteria.

BWS, Beckwith–Wiedemann syndrome; DMR, differentially methylated region; HIL, hypomethylation of imprinted loci; ID, imprinting disorder; TND, transient neonatal diabetes.

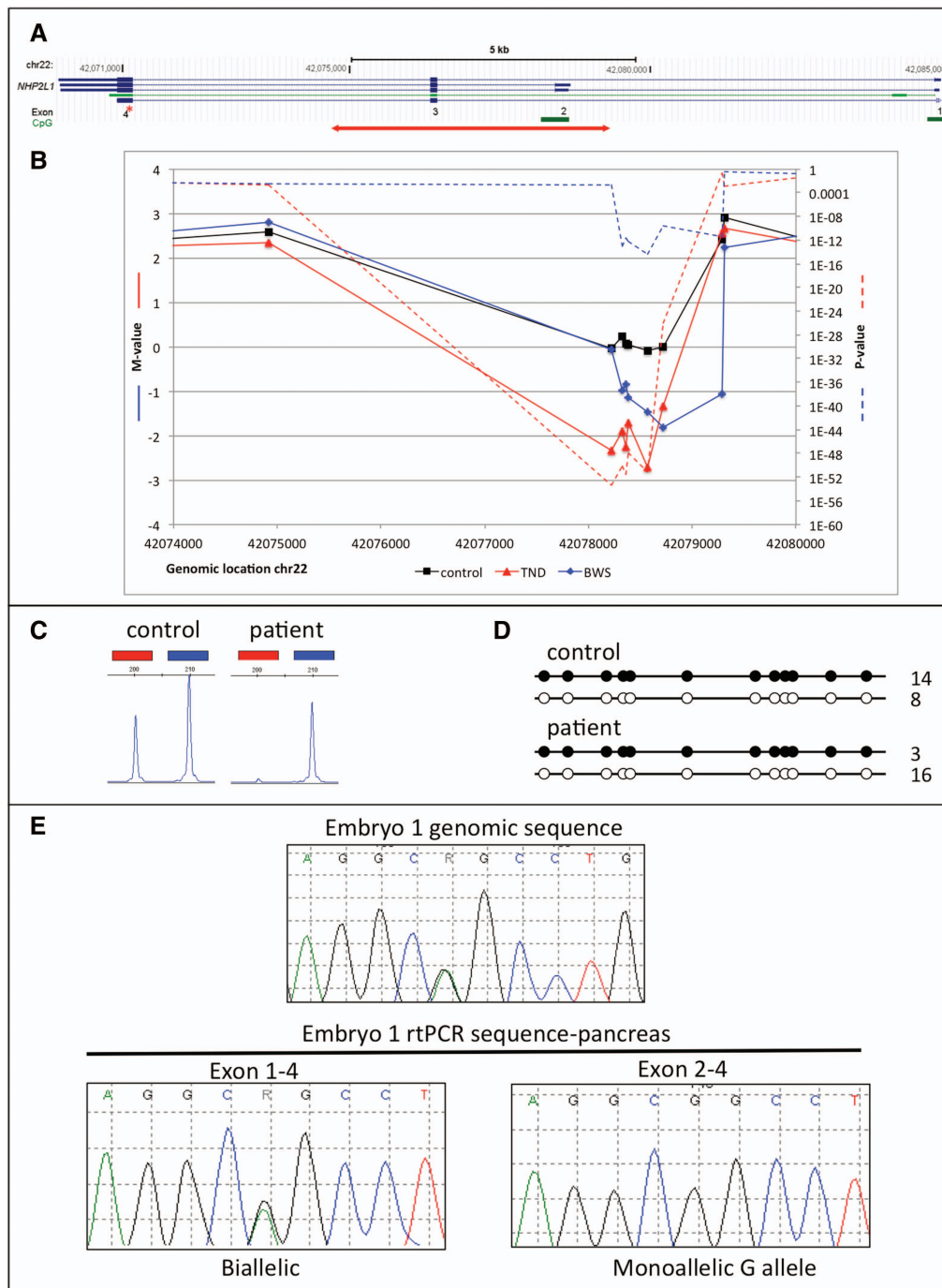


Figure 2 DNA methylation and expression analysis of *NHP2L1* in patients with Beckwith–Wiedemann syndrome (BWS) and transient neonatal diabetes (TND). (A) Screenshot from UCSC genome browser representing the *NHP2L1* gene and imprinted locus. The subregion highlighted in (B) is marked by a red double-headed arrow. Small numbers under the screenshot denote the exon numbering as used for expression analysis in (E); red asterisk indicates the position of the SNP analysed in (E). Note that *NHP2L1* is transcription from right to left with respect to genomic orientation. (B) Divergent DNA methylation between normal controls and patients, detected by methylation array. Solid lines denote M-values (left axis). Dashed lines represent p values of methylation difference between patients and controls (right axis). Black line represents normal controls; blue lines represent averaged methylation of five BWS patients; red lines represent averaged methylation of five TND patients. (C) Illustrative electropherogram from methylation-specific PCR experiment showing difference in DNA methylation between a single patient and control. Amplicons derived from methylated and unmethylated DNA are marked by red and blue lines, respectively. (D) Summary of bisulfite cloning and sequencing experiment comparing a patient with a normal control. The circles represent CpG dinucleotides within a sequence amplified after bisulfite modification, with filled and empty circles representing methylated and unmethylated DNA sequences respectively. The number to the right indicates the number of times the sequence was detected in individual clones. In no case were methylated and unmethylated CpG dinucleotides detected within a single clone. (E) Allele-specific expression analysis of *NHP2L1*. Top electropherogram represents genomic sequencing across rs8779 showing heterozygous SNP. Lower electropherograms represent sequencing of RT-PCR products from pancreatic cDNA, amplified from exons 1–4 (biallelic expression) and 2–4 (monoallelic).

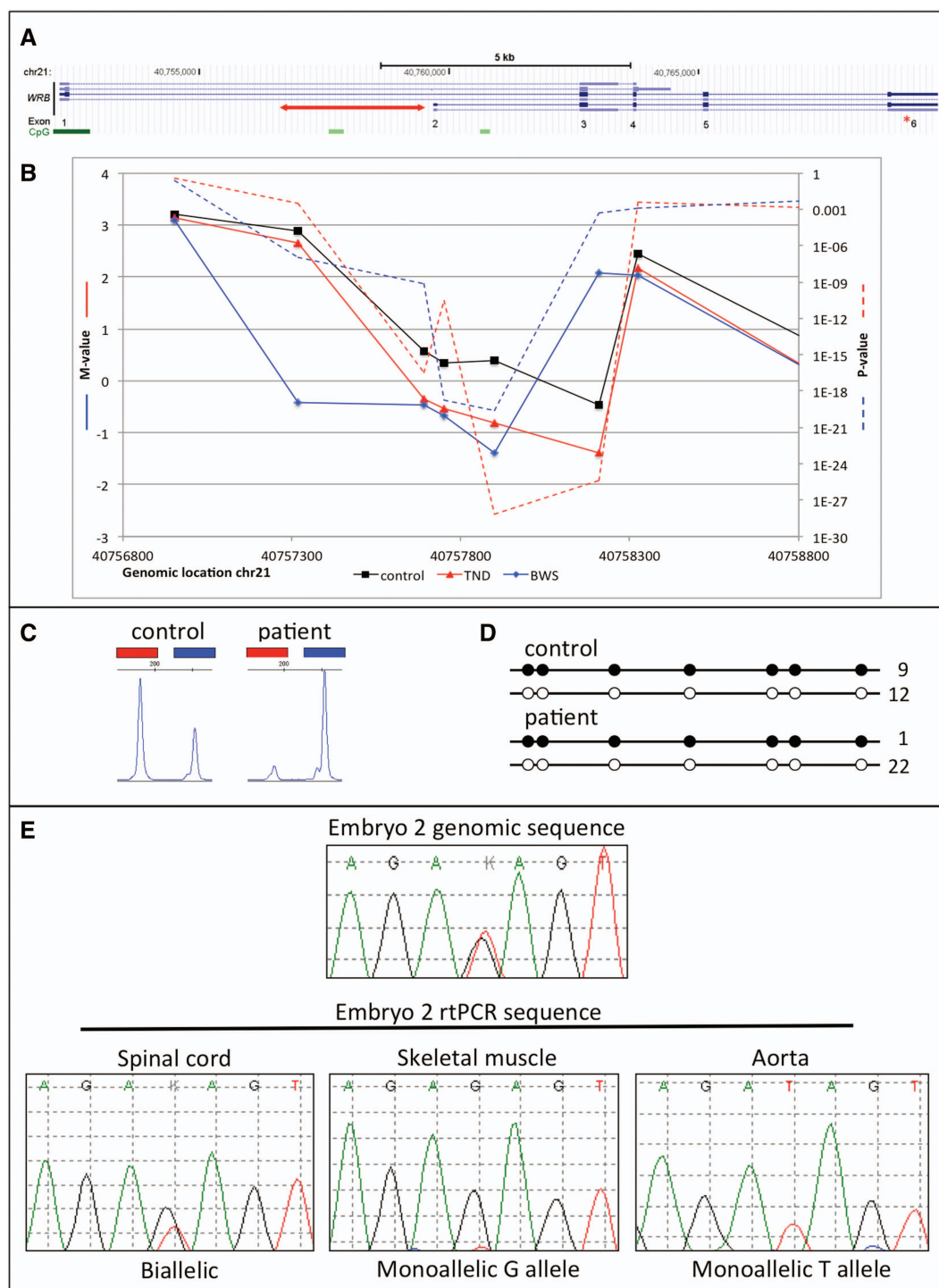


Figure 3 DNA methylation and expression analysis of *WRB* in patients with Beckwith–Wiedemann syndrome (BWS) and transient neonatal diabetes (TND). (A) Screenshot from UCSC genome browser, representing the *WRB* gene and imprinted locus. The subregion highlighted in (B) is marked by a red double-headed arrow. Small numbers under the screenshot denote the exon numbering as used for expression analysis in (E); red asterisk indicates the position of the SNP analysed in (E). (B) Divergent DNA methylation between normal controls and patients, detected by methylation array. Solid lines denote M-values (left axis). Dashed lines represent p values of methylation difference between patients and controls (right axis). Black line represents normal controls; blue lines represent averaged methylation of five BWS patients; red lines represent averaged methylation of five TND patients. (C) Illustrative electropherogram from methylation-specific PCR experiment, showing difference in DNA methylation between a single patient and control. Amplicons derived from methylated and unmethylated DNA are marked by red and blue lines, respectively. (D) Summary of bisulfite cloning and sequencing experiment comparing a patient with a normal control. The circles represent CpG dinucleotides within a sequence amplified after bisulfite modification, with filled and empty circles representing methylated and unmethylated DNA sequences, respectively. The number to the right indicates the number of times that sequence was detected in individual clones. In no case were methylated and unmethylated CpG dinucleotides detected within a single clone. (E) Allele-specific expression analysis of *WRB*. Top electropherogram represents genomic sequencing across rs1060180 showing heterozygous SNP. Lower electropherograms represent sequencing of RT-PCR amplicons in human fetal tissues as stated.

and 3, see online supplementary figure S3A). msPCR on a panel of 96 anonymised normal control samples showed methylation levels at all three loci to be stable in the normal population (SD *NHP2L1*=0.18, *WRB*=0.23 and *PPIEL*=0.22; data not shown). Analysis of complete hydatidiform mole (no methylation at maternally imprinted loci) showed complete hypomethylation in all three loci (data not shown).

DNA methylation at the candidate loci was then confirmed by msPCR in four of the five test HIL patients in each cohort (figures 2C and 3C; see online supplementary figure S3C; online supplementary table S1). For the two other patients, insufficient DNA remained for further analysis). All showed hypomethylation of at least one candidate locus: 2/4 TND-HIL patients were hypomethylated at all 3 loci, while 3/4 BWS-HIL and 1/4 TND-HIL patients showed hypomethylation at 2–3 loci. We then explored the methylation of these loci in DNA from further ID patients, including those with and without HIL, and those with hypomethylation of maternal and paternal DNA. Four of five additional TND-HIL patients and five of six additional BWS-HIL patients had hypomethylation at one or more loci, thus validating these as regions frequently affected by hypomethylation in TND-HIL and BWS-HIL patients (see online supplementary table S1). Less expected was the observation that *NHP2L1*, *WRB* and *PPIEL* candidate DMRs also showed hypomethylation in SRS-HIL patients (6/7, 4/7 and 1/7, respectively) and *WRB* hypomethylation in 1/1 PHP-HIL patient. No hypomethylation was observed at any of the loci in five patients with *ZFP57* mutations nor in nine patients with an ID affecting only one locus. This suggested that hypomethylation at these loci was restricted to HIL patients, rather than being widespread among ID patients.

Additionally, *WRB* methylation was analysed in 34 anonymised DNA samples from individuals diagnosed with Down syndrome. In all, 31 samples showed partial hypermethylation in a ratio consistent with the presence of one additional methylated allele of *WRB*; two showed partial hypomethylation consistent with one additional unmethylated allele of *WRB*; and one showed methylation equivalent to normal controls (see online supplementary figure S4). We were unable to confirm the parental origin of the additional chromosome 21 for these patients. However, given that 95% of trisomy 21 is of maternal origin,³³ we infer that this ratio of apparent hypermethylation and hypomethylation, at 31:2 Down syndrome patients (94%:6%), is consistent with DNA methylation being present on the maternal allele of *WRB*.

Parent of origin-specific methylation were investigated at *NHP2L1* and *PPIEL* candidate DMRs using methylation-specific restriction digest and sequencing. These results were consistent with maternal inheritance of the methylated allele at both candidate DMRs (see online supplementary figures S5 and S6). To further demonstrate that DNA methylation was discrete, that is, concentrated on one allele rather than homogeneously distributed, we performed bisulfite cloning and sequencing of *NHP2L1*, *WRB* and *PPIEL* DMRs. Amplicons from each candidate region were cloned and sequenced in two controls and two patients identified by msPCR as having hypomethylation. This confirmed the presence of fully-methylated and fully-unmethylated amplicons in controls, and relative hypomethylation in patient samples for all three candidate regions (figures 2D and 3D; see online supplementary figure S2D).

Validation of allele-specific expression

To determine whether the hypomethylation observed at the three candidate DMRs correlated with allele-specific expression

of the associated genes, we analysed expression of transcripts in human foetal nucleic acids. We identified informative SNPs in *NHP2L1* and *WRB* in the genomic DNA of 8–12 week embryos (we could not identify informative coding SNPs in *PPIEL*). Matched RNA from multiple tissues was reverse-transcribed and amplified by RT-PCR using isoform-specific primers.

For *NHP2L1*, monoallelic expression was observed for exon 2–4 specific transcripts and biallelic expression for exon 1–4 specific transcripts (figure 2E) in all tested tissues for four embryos (data not shown). Biallelic expression of *WRB* was observed in the majority of tissues tested with both exon 1–6 and 2–6 specific transcripts. However, sporadic monoallelic expression was observed with opposing allelic expression in the skeletal muscle and aorta of a single embryo (exon 1–6 specific primers: figure 3E), and monoallelic expression in 1/3 adrenal tissues assayed (exon 2–6 specific primers; data not shown).

DISCUSSION

The data presented here demonstrate the successful use of whole genome methylation array technology to explore the methylome in two rare epigenetically defined cohorts of patients with IDs characterised by HIL.

Our small cohort size necessitated the development of a new pipeline capable of robust analysis of small group sizes. While other statistical analyses could not significantly detect hypomethylated loci, the linear model we applied in the pipeline, with the stringent criteria, detected differential methylation robustly. These loci were validated by the evidence from the prior partial epigenetic profiling of our patient groups and low p values. Moreover, these p values were proportionate to the degree of hypomethylation predicted from the known patient epimutations. This allowed us to use the pipeline confidently to predict novel imprinted regions.

Consistent with the aim of this study, novel candidate DMRs were identified that share several attributes of imprinted genes. From the nine candidate DMRs identified, follow-up of three candidates did not validate hypomethylation in the patients analysed by 450 K methylation array. These loci showed hypomethylation in additional TND-HIL and BWS-HIL patients, but not in patients with hypomethylation restricted to one primary locus or in normal controls. Hypomethylation of all loci in individuals with SRS-HIL and *WRB* in a PHP-HIL patient expanded the range of patients observed to have hypomethylation at these regions. Additionally, allele-specific methylation and parent-specific methylation analysis was consistent with monoallelic methylation of maternal origin for all three candidate DMRs, with *NHP2L1* and *WRB* showing evidence of allele-specific expression.

It is noteworthy that patterns of hypomethylation were shared between HIL patients with divergent clinical presentations. This is a surprising observation, but consistent with a shared cause of their syndromic presentation. It has become apparent in recent years that IDs with common phenotypes are associated with multiple imprinted genes (eg, H19 and *KCNQ1OT1* in BWS, and H19 and chr7 in SRS: refs^{34–35}). It is also apparent that some patients with HIL have clinical features inconsistent with their epigenotype.^{14–36–37} There may be several reasons for this phenotype–epigenotype divergence, but the most likely is somatic mosaicism, which is common among IDs and strongly modifies clinical presentation. It is therefore possible that common underlying causes, including environmental insults, primary epimutations and trans-acting mutations, may cause HIL disorders with highly variable phenotypic features. Comprehensive epigenetic profiling may be required to

stratify HIL patients with common epimutation patterns and seek subtle clinical overlaps. Such stratification may support exome analysis for common genetic causes, and moreover identify further epimutations that may account for some of their additional clinical features. It may also be informative to compare epigenotype patterns among patients of different genetic aetiologies. In this regard, it is interesting that an epigenetic analysis of a patient whose mother had an *NLRP7* mutation showed very limited overlap of affected imprinted genes (*FAM50B*) alone with our patients, but some shared hypomethylation of non-imprinted genes which may inform differences in clinical presentation.³⁸

Of the three candidate imprinted loci described here, none has a well-defined role in either normal physiology or a disease process. *NHP2L1* is a nuclear protein which plays a role in pre-mRNA splicing as a component of the U4/U6-U5 tri-snRNP³⁹ and shows evidence of allele-specific methylation.³² Little is known about the function of *PPIEL* (pseudogene of peptidylprolyl isomerase E) but aberrant DNA methylation at *PPIEL* has previously been associated with bipolar disorder with a reported strong inverse correlation between gene expression and DNA methylation levels of *PPIEL*.⁴⁰ *WRB* encodes a basic nuclear protein of unknown function and maps to the region associated with congenital heart disease in Down syndrome.^{41 42} The clinical relevance of these loci, if any, is unknown. It is possible that these genes, or any of the others identified as hypomethylated in our study, could be associated additional clinical disorders beyond the eight IDs currently known in clinical genetics. Cardiac disorders have been reported in 9% of a TND cohort,¹³ and it is possible that analysis of further patients will reveal whether the involvement of this locus is of clinical significance.

There were several potential limitations to our study. First, whole genome methylation analysis by array is restrictive to the sequences captured on the array: many more candidate imprinted regions may have potentially been obtained from whole genome bisulfite sequencing; second, additional HIL cohorts with other IDs may have provided further candidates; third, the grouping of disease cases was necessary for statistical purposes, but may have masked the hypomethylation of less strongly-affected loci. For the candidate regions that have been identified there are further limitations to expression analysis in the form of low frequency SNPs and potentially imprinted transcript identification. DNA methylation is only one component of the cellular machinery of imprinting, and the methylation signature does not necessarily collocate with the gene(s) under its control, or as has been observed in the case of the candidate region *PPIEL*, not even residing within a CpG island.

Further work is required to exploit the findings of this study. The candidate imprinted loci identified here must be characterised to determine whether their epimutation has any bearing on clinical features in the context of HIL or in as-yet undescribed ID. These or similar patients may be more comprehensively analysed by whole genome bisulfite sequencing to increase capture of candidate genes. Greater resolution may also be obtained if a bioinformatic pipeline can be developed for statistically robust analysis of individuals, rather than groups of patients; indeed, such analysis might be the basis for a comprehensive clinical genetic diagnosis of HIL. Analysis of further patients may support accurate stratification of patient groups with common epigenetic signatures—with or without common phenotype. This in turn would support the search for candidate trans-acting gene mutations by exome analysis. Identification of common DNA motifs in hypomethylated loci may also indicate

association with common trans-acting factors (by analogy with *ZFP57*), and such motifs would be the focus for cis-acting mutations in IDs. Overall, the potential benefits are disproportionate to the rarity of the patients being analysed, and may include novel insight into the basic mechanisms of human epigenetics, as well as novel loci that may be implicated in many other disorders including Down Syndrome and bipolar disorder.

Correction notice This article has been corrected since it was published Online First. The Open Access licence should be CC-BY.

Acknowledgements We thank the High-Throughput Genomics Group at the Wellcome Trust Centre for Human Genetics (funded by Wellcome Trust grant reference 090532/Z/09/Z and MRC Hub grant G0900747 91070) for the generation of the methylation data.

Contributors LED performed laboratory work, supported by RLP, HJ and HL. FIR performed bioinformatics. GL, HA and JH provided control cohorts and data derived therefrom. DIW provided human nucleic acids. IKT accrued the patient cohort, and DJGM was the PI on the project.

Funding The cohort 'Imprinting Disorders-Finding out Why' was accrued under funding from the Newlife Foundation for Disabled Children. Funding for DNA collection and Methylation analysis of normal control samples was provided in part by the National Institutes of Health (NIH) R01 AI091905-01 (PI: Wilfried Karmaus), R01 AI061471 (PI: Susan Ewart) and R01 HL082925 (PI: S. Hasan Arshad).

Competing interests LED and FIR were funded by the Medical Research Council. DJGM is a member of the COST consortium for Imprinting disorders BM1208 (<http://www.imprinting-disorders.eu>).

Ethics approval Southampton and South West Hampshire Research Ethics committee 07/H0502/85/Wiltshire Research Ethics committee 08/H0104/15/NRES Committee South Central.

Provenance and peer review Not commissioned; externally peer reviewed.

Data sharing statement Data from this study that do not pertain to individual patients are freely available, in accordance with the principles of the funding agency, Medical Research Council UK, and can be obtained by contacting the authors.

Open Access This is an Open Access article distributed in accordance with the terms of the Creative Commons Attribution (CC BY 3.0) license, which permits others to distribute, remix, adapt and build upon this work, for commercial use, provided the original work is properly cited. See <http://creativecommons.org/licenses/by/3.0/>

REFERENCES

- Messerschmidt DM, de Vries W, Ito M, Solter D, Ferguson-Smith A, Knowles BB. Trim28 is required for epigenetic stability during mouse oocyte to embryo transition. *Science* 2012;335:1499–502.
- Seisenberger S, Peat JR, Hore TA, Santos F, Dean W, Reik W. Reprogramming DNA methylation in the mammalian life cycle: building and breaking epigenetic barriers. *Phil Trans Roy Soc Lond B* 2013;368:20110330.
- Smallwood SA, Tomizawa S, Krueger F, Ruf N, Carli N, Segonds-Pichon A, Sato S, Hata K, Andrews SR, Kelsey G. Dynamic CpG island methylation landscape in oocytes and preimplantation embryos. *Nat Genet* 2011;43:811–14.
- Peters J, Beechey C. Identification and characterisation of imprinted genes in the mouse. *Brief Funct Genomic Proteomic* 2004;2:320–33.
- Yamazawa K, Ogata T, Ferguson-Smith AC. Uniparental disomy and human disease: an overview. *Am J Med Genet* 2010;154C:329–34.
- Gregg C, Zhang J, Weissbourd B, Luo S, Schroth GP, Haig D, Dulac C. High-resolution analysis of parent-of-origin allelic expression in the mouse brain. *Science* 2010;329:643–8.
- DeVeale B, van der Kooy D, Babak T. Critical evaluation of imprinted gene expression by RNA-Seq: a new perspective. *PLoS Genet* 2012;8:e1002600.
- Schalkwyk LC, Meaburn EL, Smith R, Dempster EL, Jeffries AR, Davies MN, Plomin R, Mill J. Allelic skewing of DNA methylation is widespread across the genome. *Am J Hum Genet* 2010;86:196–212.
- Kelsey G, Bartolomei MS. Imprinted genes ... and the number is? *PLoS Genet* 2012;8:e1002601.
- Horsthemke B. Mechanisms of imprint dysregulation. *Am J Med Genet* 2010;154C:321–8.
- Eggermann T, Leisten I, Binder G, Begemann M, Spengler S. Disturbed methylation at multiple imprinted loci: an increasing observation in imprinting disorders. *Epigenomics* 2011;3:625–37.
- Poole RL, Docherty LE, Al Sayegh A, Caliebe A, Turner C, Baple E, Wakeling E, Harrison L, Lehmann A, Temple IK, Mackay DJG. Targeted methylation testing of a

- patient cohort broadens the epigenetic and clinical description of imprinting disorders. *Am J Med Genet* 2013;161A:2174–82.
- 13 Docherty LE, Kabwama S, Lehmann A, Hawke E, Harrison L, Flanagan SE, Ellard S, Hattersley AT, Shield JP, Ennis S, Mackay DJG, Temple IK. Clinical presentation of 6q24 transient neonatal diabetes mellitus (6q24 TNDM) and genotype-phenotype correlation in an international cohort of patients. *Diabetologia* 2013;56:758–62.
 - 14 Azzi S, Rossignol S, Steunou V, Sas T, Thibaud N, Danton F, Le Jule M, Heinrichs C, Cabrol S, Gicquel C, Le Bouc Y, Netchine I. Multilocus methylation analysis in a large cohort of 11p15-related foetal growth disorders (Russell Silver and Beckwith Wiedemann syndromes) reveals simultaneous loss of methylation at paternal and maternal imprinted loci. *Hum Mol Genet* 2009;18:4724–33.
 - 15 Mackay DJG, Callaway JLA, Marks SM, White HE, Acerini CL, Boonen SE, Dayanikli P, Firth HV, Goodship JA, Haemers AP, Hahnemann JMD, Kordonouri O, Masoud AF, Oestergaard E, Storr J, Ellard S, Hattersley AT, Robinson DO, Temple IK. Hypomethylation of multiple imprinted loci in individuals with transient neonatal diabetes is associated with mutations in *ZFP57*. *Nat Genet* 2008;40:949–51.
 - 16 Parry DA, Logan CV, Hayward BE, Shires M, Landolsi H, Diggle C, Carr I, Rittore C, Toutou I, Philibert L, Fisher RA, Fallahian M, Huntriss JD, Picton HM, Malik S, Taylor GR, Johnson CA, Bonthron DT, Sheridan EG. Mutations causing familial biparental hydatidiform mole implicate c6orf221 as a possible regulator of genomic imprinting in the human oocyte. *Am J Hum Genet* 2011;89:451–8.
 - 17 Van den Veyver IB, Al-Hussaini TK. Biparental hydatidiform moles: a maternal effect mutation affecting imprinting in the offspring. *Hum Reprod Update* 2006;12:233–42.
 - 18 Judson H, Hayward BE, Sheridan E, Bonthron DT. A global disorder of imprinting in the human female germ line. *Nature* 2002;416:539–42.
 - 19 Choufani S, Shapiro JS, Susiarjo M, Butcher DT, Grafodatskaya D, Lou Y, Ferreira JC, Pinto D, Scherer SW, Shaffer LG, Coullin P, Caniggia I, Beyene J, Slim R, Bartolomei MS, Weksberg R. A novel approach identifies new differentially methylated regions (DMRs) associated with imprinted genes. *Genome Res* 2011;21:465–76.
 - 20 Court F, Martin-Trujillo A, Romanelli V, Garin I, Iglesias-Platas I, Salafsky I, Guitart M, Perez de Nancarrow G, Lapunzina P, Monk D. Genome-wide allelic methylation analysis reveals disease-specific susceptibility to multiple methylation defects in imprinting syndromes. *Hum Mut* 2013;34:595–602.
 - 21 Nakabayashi K, Trujillo AM, Tayama C, Campubri C, Yoshida W, Lapunzina P, Sanchez A, Soejima H, Aburatani H, Nagae G, Ogata T, Hata K, Monk D. Methylation screening of reciprocal genome-wide UPDs identifies novel human-specific imprinted genes. *Hum Mol Genet* 2011;20:3188–97.
 - 22 Wang D, Yan L, Hu Q, Sucheston LE, Higgins MJ, Ambrosone CB, Johnson CS, Smiraglia DJ, Liu S. IMA: an R package for high-throughput analysis of Illumina's 450 K Infinium methylation data. *Bioinformatics* 2012;28:729–30.
 - 23 Boks MP, Derks EM, Weisenberger DJ, Strengman E, Janson E, Sommer IE, Kahn RS, Ophoff RA. The relationship of DNA methylation with age, gender and genotype in twins and healthy controls. *PLoS One* 2009;4:e6767.
 - 24 El-Maari O, Becker T, Junen J, Manzoor SS, Diaz-Lacava A, Schwaab R, Wienker T, Oldenburg J. Gender specific differences in levels of DNA methylation at selected loci from human total blood: a tendency toward higher methylation levels in males. *Hum Genet* 2007;122:505–14.
 - 25 Du P, Zhang X, Huang CC, Jafari N, Kibbe WA, Hou L, Lin SM. Comparison of Beta-value and M-value methods for quantifying methylation levels by microarray analysis. *BMC Bioinformatics* 2010;11:587.
 - 26 Dempster EL, Pidsley R, Schalkwyk LC, Owens S, Georgiades A, Kane F, Kalidindi S, Picchioni M, Kravariti E, Touloupoulou T, Murray RM, Mill J. Disease-associated epigenetic changes in monozygotic twins discordant for schizophrenia and bipolar disorder. *Hum Mol Genet* 2011;20:4786–96.
 - 27 Dedeurwaerder S, Defrance M, Calonne E, Denis H, Sotiriou C, Fuks F. Evaluation of the Infinium Methylation 450 K technology. *Epigenomics* 2011;3:771–84.
 - 28 Benjamini Y, Hochberg Y. Controlling the false discovery rate: a practical and powerful approach to multiple testing. *J R Stat Soc* 1995;57:289–300.
 - 29 Smyth GK. Limma: linear models for microarray data. In: Gentleman VR, Carey SD, Irazary R, Huber W. eds. *Bioinformatics and computational biology solutions using R and bioconductor*. New York: Springer, 2005:397–420.
 - 30 Crawford JR, Garthwaite PH. Single-case research in neuropsychology: a comparison of five forms of t-test for comparing a case to controls. *Cortex* 2012;48:1009–16.
 - 31 Poole RL, Leith DJ, Docherty LE, Shmela ME, Gicquel C, Temple IK, Mackay DJG. Beckwith-Wiedemann syndrome caused by maternally-inherited mutation of an OCT-binding motif in the IGF2/H19 imprinting control region, ICR1. *Eur J Hum Genet* 2012;20:240–3.
 - 32 Fang F, Hodges E, Molaro A, Dean M, Hannon GJ, Smith AD. Genomic landscape of human allele-specific DNA methylation. *PNAS USA* 2012;109:7332–7.
 - 33 Antonarakis SE. Parental origin of the extra chromosome in trisomy 21 as indicated by analysis of DNA polymorphisms. Down Syndrome Collaborative Group. *NEJM* 1991;324:872–6.
 - 34 Choufani S, Shuman C, Weksberg R. Beckwith-Wiedemann syndrome. *Am J Med Genet* 2010;154C:343–54.
 - 35 Eggermann T. Russell-Silver syndrome. *Am J Med Genet* 2010;154C:355–64.
 - 36 Boonen SE, Mackay DJ, Hahnemann JM, Docherty L, Grønskov K, Lehmann A, Larsen LG, Haemers AP, Kockaerts Y, Dooms L, Vu DC, Ngoc CT, Nguyen PB, Kordonouri O, Sundberg F, Dayanikli P, Puthi V, Acerini C, Massoud AF, Tümer Z, Temple IK. Transient neonatal diabetes, *ZFP57*, and hypomethylation of multiple imprinted loci: a detailed follow-up. *Diabetes Care* 2013;36:505–12.
 - 37 Scott RH, Douglas J, Baskcomb L, Huxter N, Barker K, Hanks S, Craft A, Gerrard M, Kohler JA, Levitt GA, Picton S, Pizer B, Ronghe MD, Williams D; Factors Associated with Childhood Tumours (FACT) Collaboration, Cook JA, Pujol P, Maher ER, Birch JM, Stiller CA, Pritchard-Jones K, Rahman N. Constitutional 11p15 abnormalities, including heritable imprinting center mutations, cause nonsyndromic Wilms tumor. *Nat Genet* 2008;40:1329–34.
 - 38 Beygo J, Ammerpohl O, Gritzan D, Heitmann M, Rademacher K, Richter J, Caliebe A, Siebert R, Horsthemke B, Buiting K. Deep bisulfite sequencing of aberrantly methylated loci in a patient with multiple methylation defects. *PLOS ONE* 2013;8:e76953.
 - 39 Liu S, Rauhut R, Vornlocher HP, Luhrmann R. The network of protein-protein interactions within the human U4/U6.U5 tri-snRNP. *RNA* 2006;12:1418–30.
 - 40 Kuratomi G, Iwamoto K, Bundo M, Kusumi I, Kato N, Iwata N, Ozaki N, Kato T. Aberrant DNA methylation associated with bipolar disorder identified from discordant monozygotic twins. *Mol Psych* 2008;13:429–41.
 - 41 Egeo A, Mazzocco M, Sotgia F, Arrigo P, Oliva R, Bergonon S, Nizetic D, Rasore-Quartino A, Scartezzini P. Identification and characterization of a new human cDNA from chromosome 21q22.3 encoding a basic nuclear protein. *Hum Genet* 1998;102:289–93.
 - 42 Murata K, Degmetich S, Kinoshita M, Shimada E. Expression of the congenital heart disease 5/tryptophan rich basic protein homologue gene during heart development in medaka fish, *Oryzias latipes*. *Dev Growth Differ* 2009;51:95–107.
 - 43 Yu Y, Xu F, Peng H, Fang X, Zhao S, Li Y, Cuevas B, Kuo WL, Gray JW, Siciliano M, Mills GB, Bast RC Jr. NOEY2 (ARHI), an imprinted putative tumor suppressor gene in ovarian and breast carcinomas. *PNAS USA* 1999;96:214–9.
 - 44 Zhang A, Skaar DA, Li Y, Huang D, Price TM, Murphy SK, Jirtle RL. Novel retrotransposed imprinted locus identified at human 6p25. *NAR* 2011;39:5388–400.
 - 45 Sharp AJ, Migliaiaccia E, Dupre Y, Stathaki E, Sailani MR, Baumer A, Schinzel A, Mackay DJ, Robinson DO, Cobellis G, Cobellis L, Brunner HG, Steiner B, Antonarakis SE. Methylation profiling in individuals with uniparental disomy identifies novel differentially methylated regions on chromosome 15. *Genome Res* 2010;20:1271–8.
 - 46 Noguer-Dance M, Abu-Amro S, Al-Khtib M, Lefevre A, Coullin P, Moore GE, Cavaillat J. The primate-specific microRNA gene cluster (C19MC) is imprinted in the placenta. *Hum Mol Genet* 2010;19:3566–82.
 - 47 Pollard KS, Serre D, Wang X, Tao H, Grundberg E, Hudson TJ, Clark AG, Frazer K. A genome-wide approach to identifying novel-imprinted genes. *Hum Genet* 2008;122:625–34.
 - 48 Li J, Bench AJ, Vassiliou GS, Fourouclas N, Ferguson-Smith AC, Green AR. Imprinting of the human *L3MBTL* gene, a polycomb family member located in a region of chromosome 20 deleted in human myeloid malignancies. *PNAS USA* 2004;101:7341–6.

Corrections

Louise E Docherty, Faisal I Rezwan, Rebecca L Poole, *et al.* Genome-wide DNA methylation analysis of patients with imprinting disorders identifies differentially methylated regions associated with novel candidate imprinted genes. *J Med Genet* 2014;**51**:229–38. doi:10.1136/jmedgenet-2013-102116. The Open Access licence should be CC-BY.



CrossMark

J Med Genet 2014;**51**:478. doi:10.1136/jmedgenet-2013-102116corr1

Supplementary Figure 1: HIL Patient cluster analysis. Clustering of 5 TND-HIL samples with 221 control samples and 5 BWS-HIL with 245 samples respectively, while including and excluding probes from X and Y chromosomes. A) and C) show samples clustered with all chromosomes for TND-HIL and BWS-HIL respectively (cluster by gender). B) and D) show clustering of TND-HIL and BWS-HIL patient groups after the removal of X and Y chromosome probes (samples no longer cluster by gender).

Supplementary Figure 2: Detection of DNA methylation within *PLAGL1* locus in patients with BWS and TND.

A) Modified screengrab from UCSC genome browser, representing the *PLAGL1* gene. The sub-regions highlighted in the panels below are marked by red double-ended arrows. B) methylation of *PLAGL1* imprinting control region measured using Illumina 450k array in patients versus controls. Solid lines denote M-values (left axis: methylation level expressed as a logarithmic ratio, with +4, 0, and -4 equivalent to hypermethylation, hemimethylation and hypomethylation respectively). Dashed lines represent P-values of methylation difference between patients and controls (right axis). Black line represents 221 normal controls; blue lines represent averaged methylation of five BWS patients; red lines represent averaged methylation of five TND patients. C) DNA methylation of *PLAGL1* non-imprinted CpG island. As above, solid lines represent M-values, and dashed lines represent P values of methylation difference between patients and controls, with black, blue and red lines representing control, BWS and TND patients respectively.

Supplementary Figure 3: DNA methylation analysis of *PPIEL* in patients with BWS and TND.

A: screengrab from UCSC genome browser, representing the *PPIEL* locus and imprinted locus. The sub-region highlighted in the panel below is marked by a red double-ended arrow. Note that *PPIEL* is transcription from right to left with respect to genomic orientation. B: divergent DNA methylation between normal controls and patients, detected by methylation array. Solid lines denote M-values (left axis). Dashed lines represent P-values of methylation difference between patients and controls (right axis). Black line represents normal controls; blue lines represent averaged methylation of five BWS patients; red lines represent averaged methylation of five TND patients. C: illustrative electropherogram from methylation-specific PCR experiment, showing difference in DNA methylation between a single patient and control. Amplicons derived from methylated and unmethylated DNA are marked by red and blue lines, respectively. D: summary of bisulphite cloning and sequencing experiment comparing patients and controls. The circles represent CpG dinucleotides within a sequence amplified after bisulphite modification, with filled and empty circles representing methylated and unmethylated DNA sequences respectively. The number to the right indicates the number of times that sequence

was detected in individual clones. In no case were methylated and unmethylated CpG dinucleotides detected within a single clone.

Supplementary Figure 4: DNA methylation analysis of *WRB* in samples from individuals with trisomy 21.

The images in the left panels are illustrative electropherograms from one methylation-specific PCR experiment, showing the differences in DNA methylation between control DNA samples and groups of samples from individuals with trisomy 21 (T21). Amplicons derived from methylated and unmethylated DNA are marked by red and blue lines, respectively. A: normal controls, B and C, DNA of individuals diagnosed with T21, showing hypermethylation and hypomethylation respectively. The figures to the right represent normalised ratios of unmethylated to methylated peak heights. Individual DNA samples were tested in duplicate, the results averaged, and then normalised to the average methylation across seven normal controls. The ratio of the unmethylated and methylated amplicons reflects that of the source DNA, such that a twofold change of peak height ratio is equivalent to a twofold excess of its source DNA. Of 34 samples from individuals diagnosed with T21, 31 showed partial hypermethylation, 2 partial hypomethylation, and one showed methylation equivalent to controls (not shown).

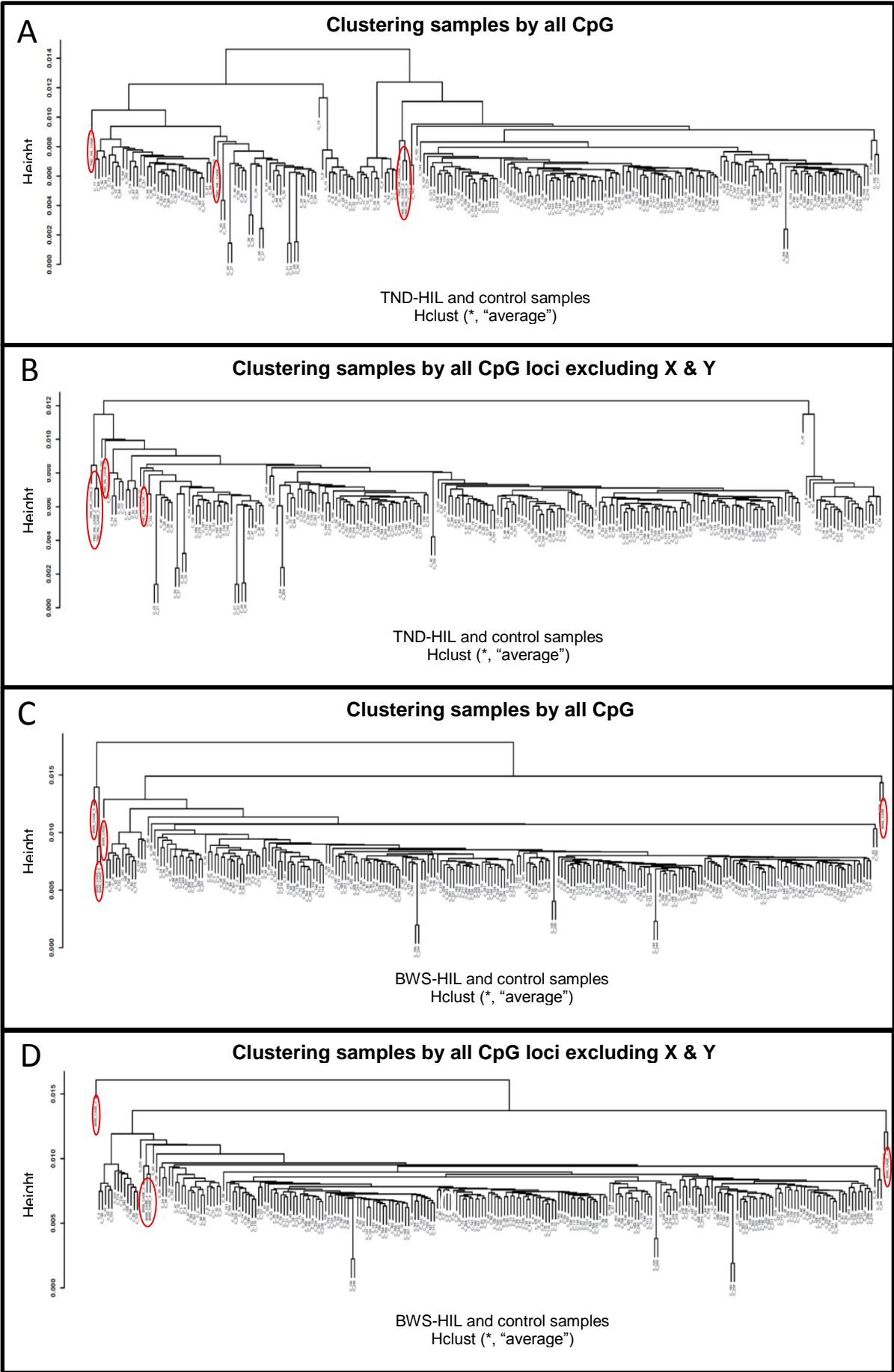
Supplementary Figure 5: Parent of origin methylation analysis of *NHP2L1* differentially-methylated region

Panels A and B show sequencing electropherograms from the mother, father and child of a trio, with the child showing heterozygous inheritance of rs6519270 (A/G: MAF 0.38). For the offspring, the upper electropherogram illustrates (heterozygous) genomic sequence, and the lower electropherogram shows DNA amplified after restriction with BstUI, which digests methylated DNA. Panel A: maternally-inherited G allele unaffected by BstUI digestion, indicating maternal methylation; Panel B: maternally-inherited A allele unaffected by BstUI digestion, indicating maternal methylation; DNA methylation is associated with parent of origin, not snp allele.

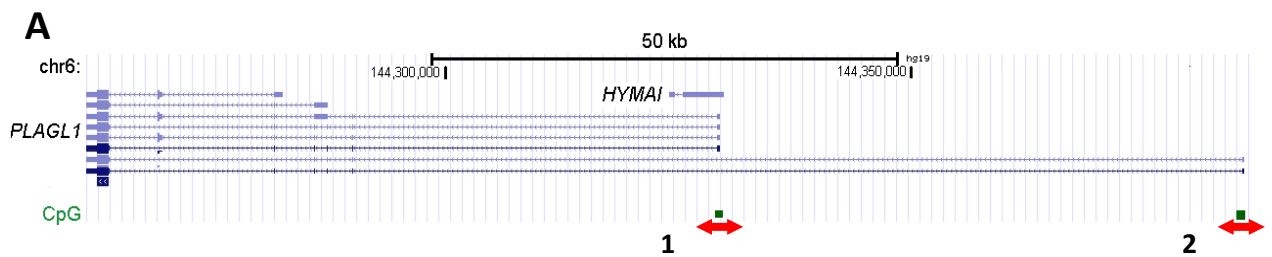
Supplementary Figure 6: Parent of origin methylation analysis of *PPIEL* differentially-methylated region

Panels A and B show sequencing electropherograms from the mother, father and child of a trio, with the child showing heterozygous inheritance of rs138909742 (G/-: MAF 0.15). For the offspring, the upper electropherogram illustrates (heterozygous) genomic sequence, and the lower electropherogram shows DNA amplified after restriction with McrBc, which digests unmethylated DNA. Panel A: paternally-inherited (deleted) allele unaffected by McrBc digestion, indicating maternal methylation; Panel B: paternally-inherited G allele unaffected by McrBc digestion, indicating maternal methylation; DNA methylation is associated with parent of origin, not snp allele.

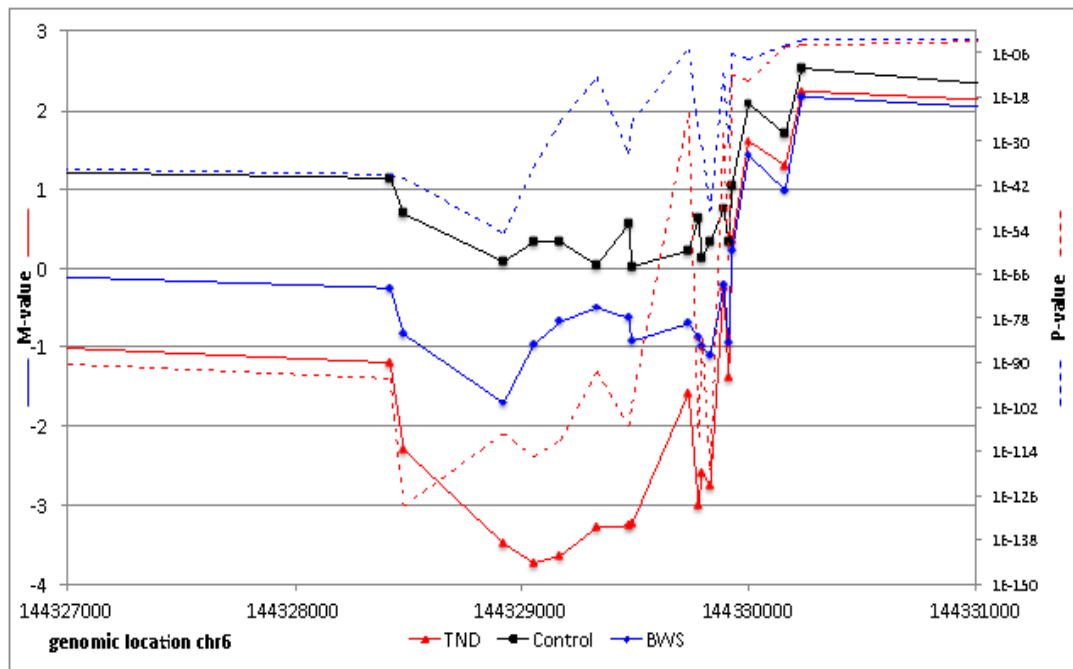
Supplementary Figure 1: HIL Patient cluster analysis.



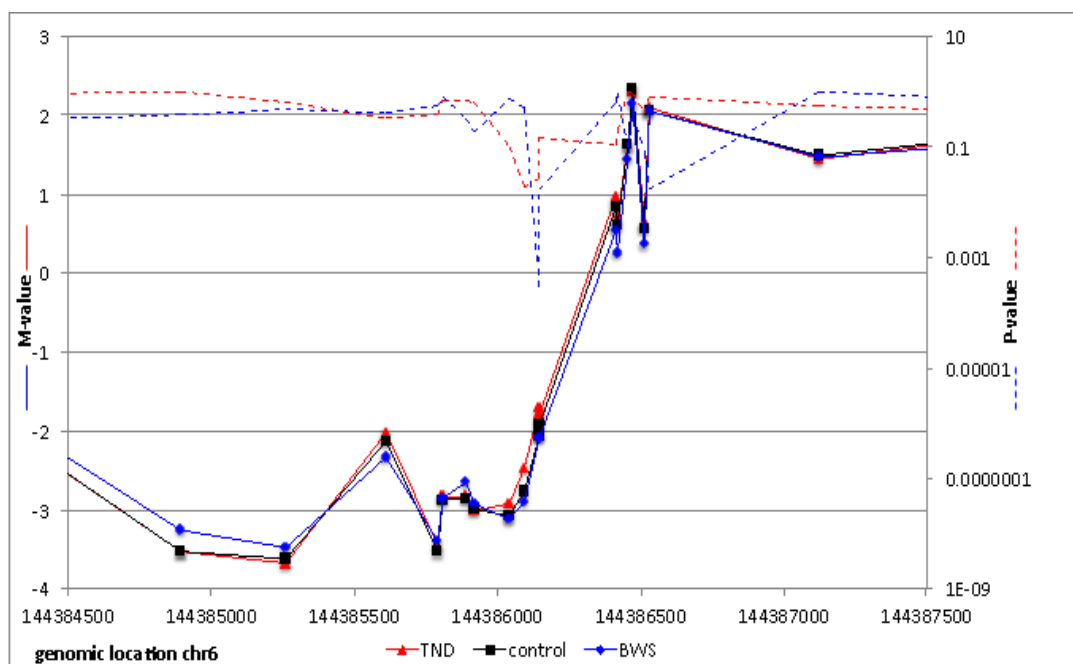
Supplementary Figure 2: Detection of DNA methylation within *PLAGL1* locus in patients with BWS and TND.



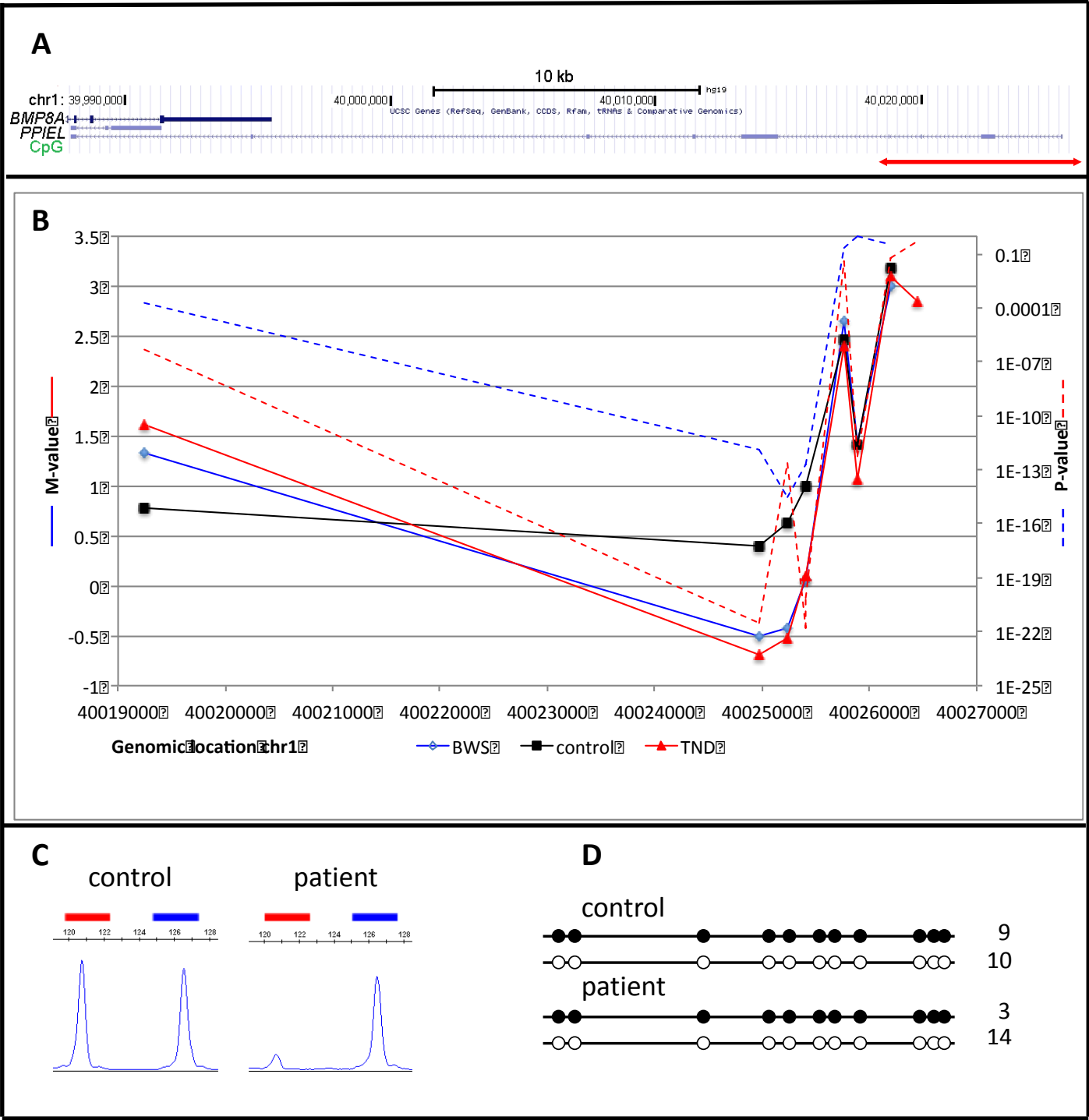
B 1: *PLAGL1* imprinted CpG



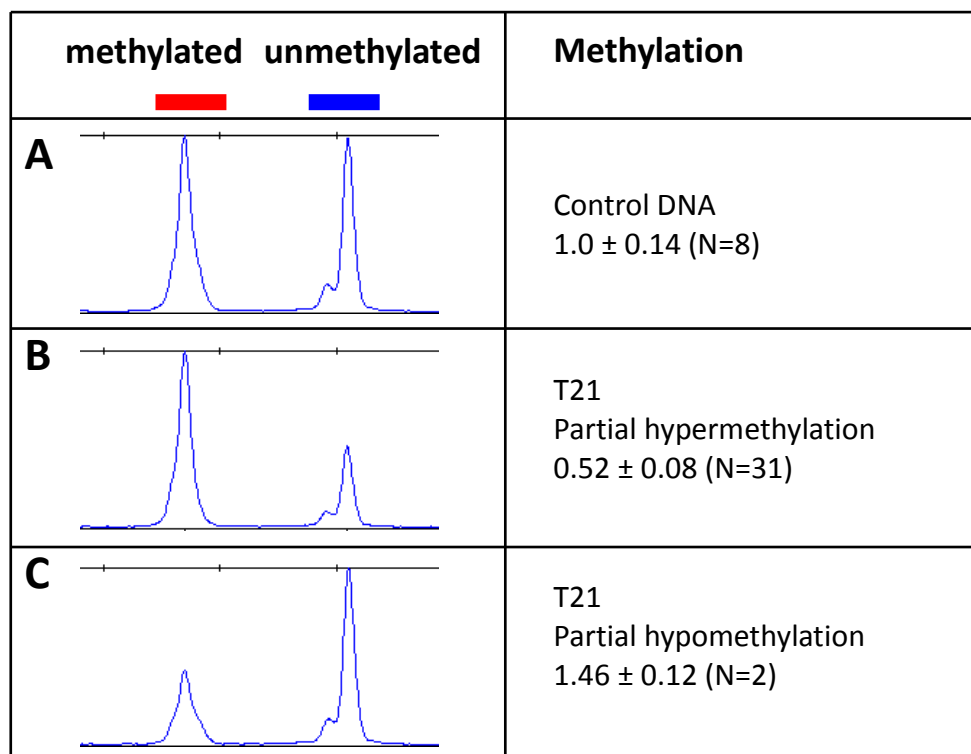
C 2: *PLAGL1* non-imprinted CpG



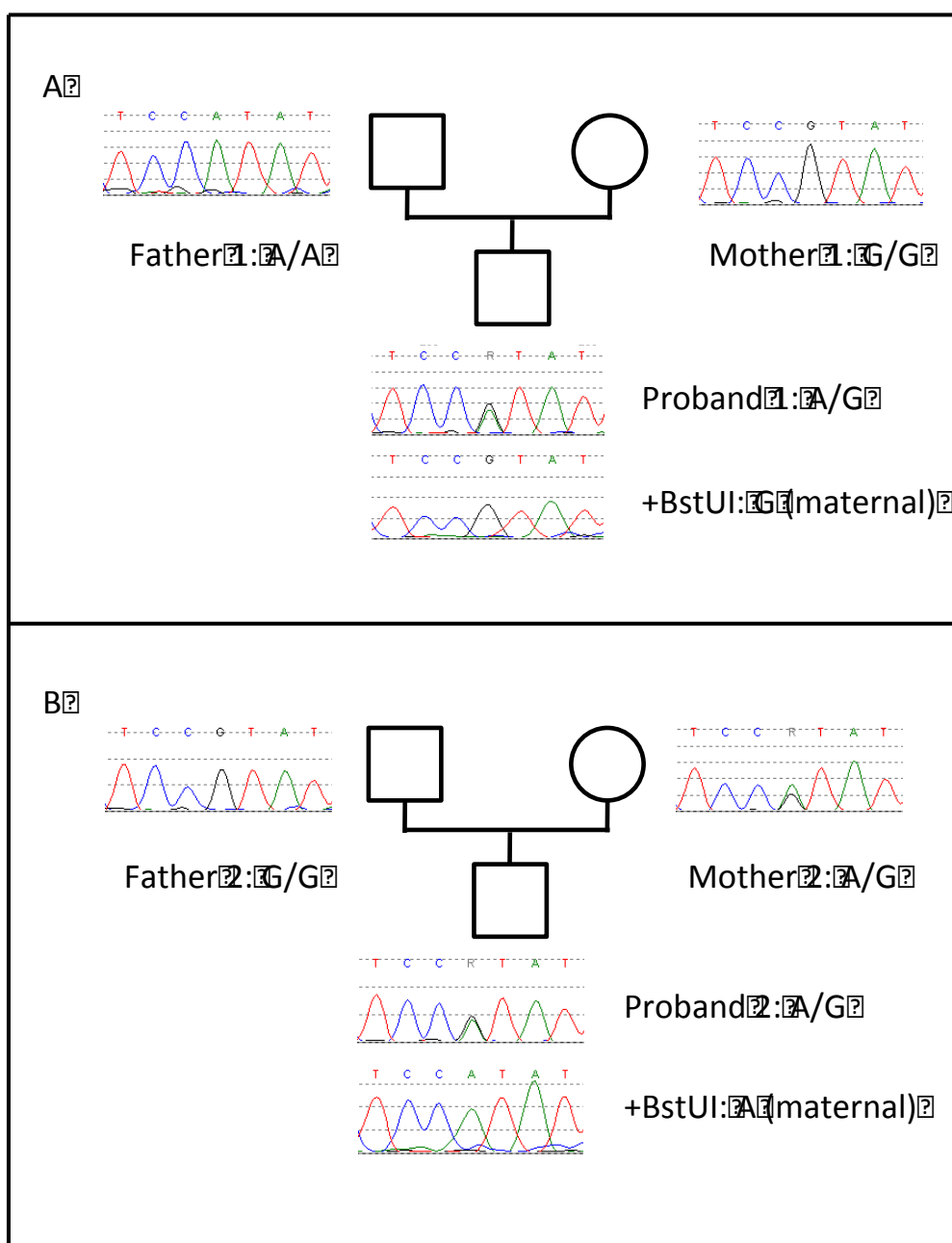
Supplementary Figure 3: DNA methylation analysis of *PPIEL* in patients with BWS and TND.



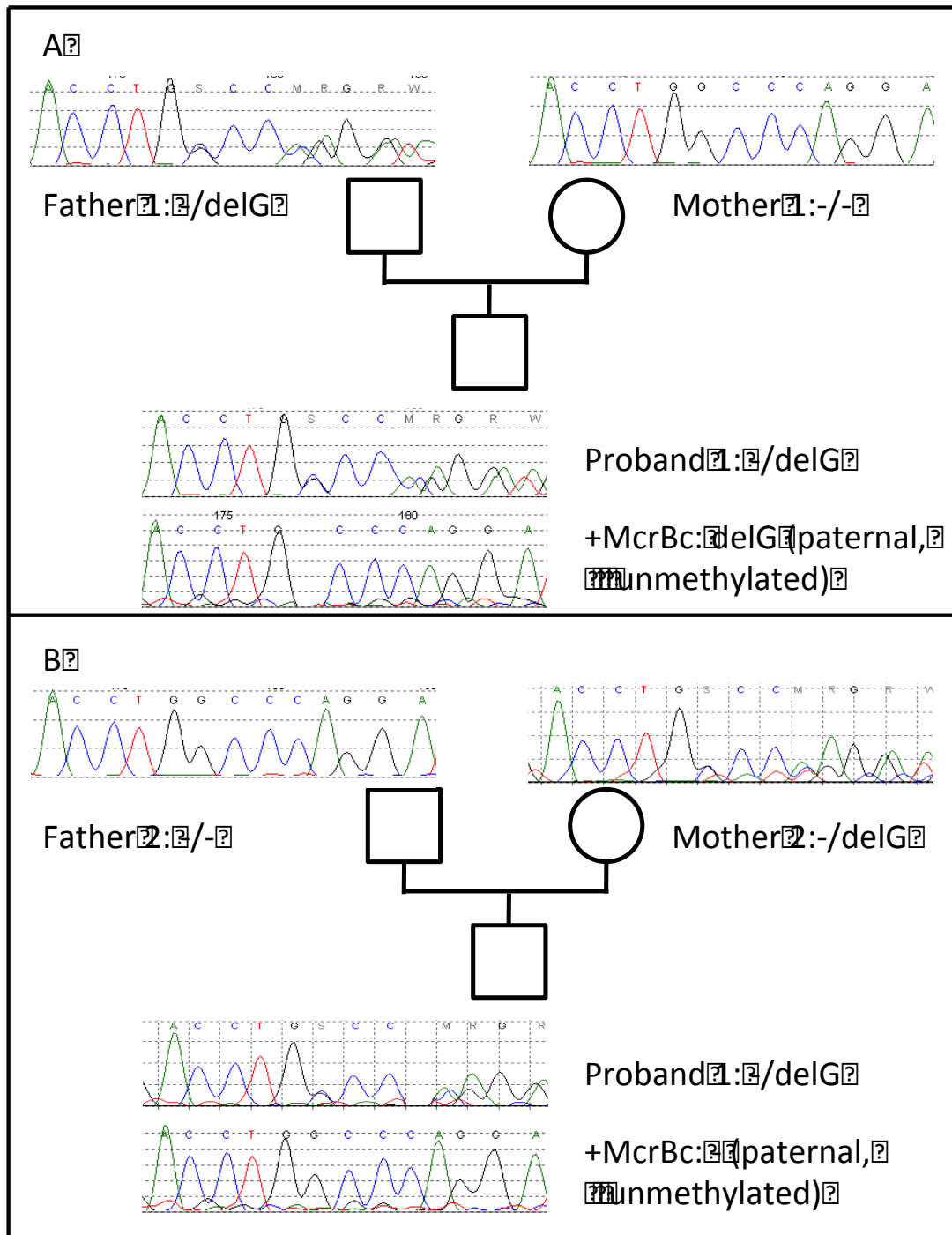
Supplementary Figure 4: DNA methylation analysis of *WRB* in samples from individuals with trisomy 21.



Supplementary Figure 5: Parent of origin methylation analysis of *NHP2L1* differentially-methylated region



Supplementary Figure 6: Parent of origin-specific methylation analysis of *PPIEL* differentially-methylated region



DNA methylation at differentially methylated loci was estimated by methylation-specific PCR. A methylation ratio of 1 is equivalent to hemizygous methylation, as seen in normal controls; a ratio of 2 indicates twofold excess of unmethylated over methylated template; complete indicates no detectable methylated amplicon. Broadly the intensity of blue shading reflects the severity of hypomethylation. Green boxes indicate complete hypermethylation. A dash indicates no data, normally because insufficient DNA preventing completion of all testing. Column headers indicate the loci tested and their genomic locations. Rows denote individual patients, grouped by their presenting disorder. Asterisks denote those patients whose DNA – on the basis of this targeted analysis – was included in methylome array analysis.

[illegible]

Supplementary Table 2: Distribution of probes of Human methylation 450K Bead Chip before and after initial quality control (QC)

Annotation	Before QC	TND-HIL after QC	BWS-HIL after QC
Island	150254	118348	109725
Shelf	47144	38927	36431
Shore	112067	93470	89275
Non-CpG	176112	146528	1378890
Total	485577	397273	373321

Supplementary Table 3: primers for DNA methylation and expression analysis of novel loci included in this report. For bisulphite-specific primers, the genomic template location in hg19 is provided; further information, and assay conditions, will be supplied on request.

Methylation-specific PCR							
DMR	Chr	Chromosomal location GRCh37	Methylated allele	Unmethylated allele size	Methylated primer	Unmethylated primer	Universal FAM labelled primer
PPIEL	1p34.3	chr1:40,025,245-40,025,376	120	126	CGGTGCGGGTTTTCGGCGGAAGC	TGGGGTATGGTGTGGGTTTTGGTGAAGT	CACCCCCAACTCAATCTTAACACTACCTAC
WRB	21q22.2	chr21:40,757,866-40,758,068	198	205	CCCTACGAACTACACGCACTACGCAAACG	CAAAATCCCTACAAACTACACACTACACAAACA	GGATAATTTAGAAAAAGTTGAATTTTAAAGGG
NHP2L1	22q13.2	chr22:42,078,073-42,078,275	199	209	CATCGTATATAACGTACGAATCGCG	CATATCACCATCATATATAACATACAAATCACA	GTTGTAAAAAAAYGGAAGGAGGAAAAGGTAGGTG
Bisulphite sequencing							
			No. CGs	Product size			
PPIEL		chr1:40,025,294-40,025,441	11	147	GATTTAAAGGAGATGTTTTGTTT	ACACCACCCTACCCTTTATAAACC	
WRB		chr21:40,757,925-40,758,057	7	132	AAAAAGTTGAATTTTAAAGGGTAT	CCCCAAAACATAATAAACTAAAT	
NHP2L1		chr22:42,078,182-42,078,353	12	171	GGTTTGGTGGGATTATTATTTA	ATTCTACTAAACCATTATCTCC	
Allele-specific expression							
				SNP	Forward	Reverse	RT-PCR
WRB		chr21:40,768,900-40,769,358	Genomic exon 6	rs1060180 G/T G=0.335, r13230 A/G A=0.331	CGGATTTCTCTTCTAGCTTAAATC	GTCAATTAGTGTGTTCTTTTAACC	
			RT-PCR		Exon 1f GATGAGCTCAGCCGCGGCCGACCAC	Exon 2f GGATCTGATTATTGTGTGCCAGGC	Exon 1f-6r: Exon 2f-6r
NHP2L1		chr22:42,070,171-42,070,376	Genomic exon 4	RS8779 A/G A=0.160	GGTAATGTGATGTTGATGTTCTCC	CTTCCTGGAATCCTTCATGCCAGC	
			RT-PCR		Exon 1f GCTTCTGAACGTCAGCTGCGCTC	Exon 2f GGCAGCAGACCGTCCAAACCGACAC	Exon 1f-4r: Exon 2f-4r

Supplementary Table 4: **BWS-HIL candidate Hypomethylated loci**- p-value of $> 1.33 \times 10^{-7}$ (0.05 divided by the number of statistical tests), M value between +1 and -1 (equivalent to a beta value of 0.3-0.7) filters were applied. Loci were removed with an average of > 2000 nt between adjacent probes (ie probably coincidental) were eliminated.

This gives: 23 new loci with 64 probes,
7 published loci with 80 probes,
4 clinical loci with 86 probes

CHR	MAPINFO	span of probes (bp)	number of probes	UCSC gene name	Adjust Pval	M-value Difference	Mean BWS M-value	Mean control M-value	Relation to UCSC CpG island	Probe ID
1	11986394	3	2	KIAA2013;KIAA2013	8.24E-09	-0.4870	-0.4117	0.0753	Island	cg01061626
1	11986397			KIAA2013;KIAA2013	6.32E-10	-0.4957	-0.2895	0.2062	Island	cg11345438
1	38513489	152	2	POU3F1	2.07E-09	-0.4669	-0.6455	-0.1786	Island	cg17791651
1	38513641			POU3F1	2.24E-10	-0.4331	-0.7260	-0.2929	Island	cg12622182
1	40024971	440	3	LOC728448	1.24E-12	-0.9013	-0.5047	0.3966	NA	cg10243676
1	40025232			LOC728448	2.99E-15	-1.0440	-0.4204	0.6236	NA	cg11704876
1	40025411			LOC728448	1.95E-13	-0.9259	0.0675	0.9934	NA	cg22862450
2	233251770	3	2	ECEL1P2	6.92E-16	-1.3397	-0.3721	0.9676	Island	cg13138089
2	233251773			ECEL1P2	1.94E-17	-1.3133	-1.0124	0.3009	Island	cg02812891
4	6107021	318	4	JAKMIP1;JAKMIP1	7.46E-09	-0.8846	-0.6271	0.2575	N_Shore	cg18994250
4	6107280			JAKMIP1;JAKMIP1	3.55E-13	-0.8418	-1.1585	-0.3167	Island	cg23166781
4	6107320			JAKMIP1;JAKMIP1	1.80E-10	-0.5965	-1.0934	-0.4969	Island	cg06231140
4	6107339			JAKMIP1;JAKMIP1	8.35E-12	-0.7988	-0.8909	-0.0921	Island	cg22098660
5	139040820	29	2	CXXC5	8.35E-08	-0.7455	-1.3319	-0.5864	Island	cg14871225
5	139040849			CXXC5	1.78E-08	-0.8799	-1.2452	-0.3653	Island	cg20455854
7	138348774	669	3	SVOPL;SVOPL	1.07E-36	-1.6818	-1.9755	-0.2937	N_Shore	cg05719902
7	138349158			SVOPL;SVOPL	1.13E-19	-1.7825	-1.4393	0.3432	Island	cg10184328
7	138349443			SVOPL;SVOPL	8.71E-35	-2.8124	-2.6469	0.1654	Island	cg23085143
8	21905599	157	2	FGF17	1.03E-13	-1.4795	-1.6067	-0.1272	Island	cg03025830
8	21905756			FGF17	8.96E-08	-0.7500	-1.6532	-0.9031	Island	cg11707219
8	37605517	266	4	LOC728024;ERLIN2	3.59E-19	-1.0975	-1.3129	-0.2153	NA	cg13346869
8	37605552			LOC728024;ERLIN2	5.78E-36	-1.0425	-1.5611	-0.5186	NA	cg05020125
8	37605717			LOC728024;ERLIN2	1.55E-25	-1.3168	-1.2730	0.0438	NA	cg21505509
8	37605783			LOC728024;ERLIN2	1.83E-26	-1.1945	-1.2196	-0.0252	NA	cg08247852
8	61626646	186	2	CHD7	4.92E-08	-0.6506	-0.4283	0.2223	Island	cg12844324
8	61626832			CHD7	1.65E-08	-0.5702	0.3021	0.8722	Island	cg20648501
8	145025059	2889	3	PLEC1;PLEC1;PLEC1;PL	2.47E-11	-1.0859	-1.7324	-0.6465	Island	cg15628518
8	145025064			PLEC1;PLEC1;PLEC1;PL	3.11E-11	-0.7351	-1.0492	-0.3141	Island	cg19893585
8	145027948			PLEC1;PLEC1;PLEC1;PL	5.33E-08	-0.7824	-1.6012	-0.8188	Island	cg24507266
9	84302344	1014	2	TLE1	1.96E-21	-0.7488	-1.5317	-0.7830	Island	cg06358300
9	84303358			TLE1;TLE1	1.13E-37	-1.2795	-1.5884	-0.3089	Island	cg20926353
9	98075481	11	2	FANCC	8.29E-58	-2.1983	-2.0879	0.1104	Island	cg14127626
9	98075492			FANCC	5.50E-47	-1.7595	-2.1661	-0.4067	Island	cg21891967
10	27702774	603	4	PTCHD3	3.47E-08	-0.8878	-0.5343	0.3536	Island	cg02402587
10	27703247			PTCHD3;PTCHD3	3.32E-10	-0.9880	-1.0256	-0.0375	Island	cg27363617
10	27703336			PTCHD3	1.28E-07	-0.8418	0.0886	0.9304	Island	cg00632657
10	27703377			PTCHD3	2.89E-08	-0.7900	-0.0224	0.7675	Island	cg15283904
17	7832909	328	3	KCNAB3	6.61E-15	-1.3244	-0.9855	0.3389	Island	cg23365801
17	7833163			KCNAB3	1.61E-13	-1.5717	-0.5974	0.9742	Island	cg27162435
17	7833237			KCNAB3	1.40E-12	-1.6540	-1.0194	0.6346	N_Shore	cg14918082
17	9729250	174	3	GLP2R	4.20E-11	-0.6233	-0.2592	0.3641	NA	cg07669517
17	9729422			GLP2R	4.68E-13	-0.8275	-0.3941	0.4334	NA	cg14783904
17	9729424			GLP2R	3.19E-12	-0.7427	0.0571	0.7998	NA	cg20261915
17	26708366	407	2	SARM1	7.85E-10	-0.5969	-1.5201	-0.9232	Island	cg14854355
17	26708773			SARM1	6.02E-16	-0.8757	-0.8363	0.0393	Island	cg13895343
17	46685292	61	3	HOXB7	4.68E-08	-1.0272	-0.6723	0.3549	Island	cg18773260
17	46685327			HOXB7	2.53E-13	-1.3283	-0.5454	0.7830	Island	cg11041817
17	46685353			HOXB7	3.26E-09	-1.6486	-0.8443	0.8043	Island	cg23669081
17	79881468	75	3	MAFG;MAFG	5.36E-15	-0.9834	-1.8562	-0.8728	S_Shore	cg10909080
17	79881523			MAFG;MAFG	6.00E-15	-1.5152	-1.9696	-0.4543	S_Shore	cg22193912
17	79881543			MAFG;MAFG	6.41E-08	-0.9052	-1.1028	-0.1975	S_Shore	cg01543184
18	77905355	592	3	LOC100130522;LOC10	6.05E-15	-1.2277	-1.7406	-0.5129	Island	cg16737533
18	77905408			LOC100130522;LOC10	4.69E-08	-1.2622	-1.9366	-0.6744	Island	cg19774868
18	77905947			LOC100130522;LOC10	2.44E-16	-0.8223	-1.5240	-0.7017	S_Shore	cg18687533
19	54485321	6	2	CACNG8;MIR935	1.72E-12	-0.7095	-0.2585	0.4510	Island	cg07785717
19	54485327			CACNG8;MIR935	1.55E-11	-0.7600	-0.2274	0.5326	Island	cg18055623
21	40757899	309	2	WRB	3.97E-16	-0.7353	-0.6770	0.0583	Island	cg26710963
21	40758208			WRB;WRB	6.45E-17	-0.5600	-1.3801	-0.8202	S_Shore	cg09916765
22	42078217	506	6	NHP2L1;NHP2L1	8.11E-11	-0.7199	-0.9742	-0.2543	Island	cg18152773
22	42078330			NHP2L1;NHP2L1	1.42E-09	-0.8472	-0.8413	0.0058	Island	cg05871614
22	42078365			NHP2L1;NHP2L1;NHP2	4.97E-10	-0.8749	-1.1455	-0.2706	Island	cg22083753
22	42078567			NHP2L1;NHP2L1	4.54E-12	-1.2019	-1.4647	-0.2628	S_Shore	cg08686092
22	42078707			NHP2L1;NHP2L1	9.87E-08	-1.1120	-1.8133	-0.7014	S_Shore	cg11677105
22	42078723			NHP2L1;NHP2L1	2.42E-09	-0.6675	-1.0542	-0.3867	S_Shore	cg11536612
Novel 64 probes		23 loci								
1	68512539	4734	21	DIRAS3	1.86E-12	-0.6872	-1.4480	-0.7608	N_Shore	cg03641225
1	68512650			DIRAS3	2.54E-12	-1.0290	-0.0707	0.9583	Island	cg24871743
1	68512777			DIRAS3	1.45E-16	-0.9303	-0.6661	0.2642	Island	cg22901840
1	68512807			DIRAS3	3.37E-13	-0.9635	-0.2877	0.6758	Island	cg20149168
1	68512845			DIRAS3	1.03E-09	-0.5282	-0.4799	0.0483	Island	cg13697378

1	68512971		DIRAS3	1.41E-11	-0.8792	-0.8191	0.0601 Island	cg09118625
1	68513063		DIRAS3	1.99E-09	-0.5020	-0.7864	-0.2844 S_Shore	cg21808053
1	68515872		DIRAS3	6.20E-09	-0.3738	-0.8896	-0.5157 N_Shore	cg17943391
1	68516080		DIRAS3	2.17E-17	-0.6964	-0.9436	-0.2473 N_Shore	cg12070746
1	68516138		DIRAS3	3.26E-17	-0.8134	-1.1615	-0.3480 N_Shore	cg25755905
1	68516272		DIRAS3;DIRAS3	2.10E-17	-0.7328	-0.5634	0.1694 Island	cg22500004
1	68516374		DIRAS3;DIRAS3	5.16E-14	-0.8107	-0.8687	-0.0580 Island	cg19694923
1	68516453		DIRAS3;DIRAS3	1.09E-18	-0.7827	-0.9485	-0.1657 Island	cg05392265
1	68516463		DIRAS3	1.64E-15	-0.6819	-0.7191	-0.0372 Island	cg06191076
1	68516465		DIRAS3	5.74E-16	-0.8946	-0.3464	0.5481 Island	cg16148270
1	68516518		DIRAS3	3.98E-13	-0.6784	-0.8956	-0.2172 N_Shore	cg13208159
1	68516627		DIRAS3	2.80E-10	-0.5093	-0.6077	-0.0984 N_Shore	cg12986021
1	68517177		DIRAS3	9.06E-23	-0.9136	-0.7105	0.2031 N_Shore	cg27545611
1	68517205		DIRAS3	3.96E-27	-1.2098	-1.2133	-0.0035 N_Shore	cg16148134
1	68517255		DIRAS3	2.02E-23	-0.7522	-0.9250	-0.1728 Island	cg13605615
1	68517273		DIRAS3	2.00E-26	-1.1904	-0.9443	0.2461 Island	cg10038185
6	3849235	583	17 FAM50B	1.08E-10	-0.6279	-0.9314	-0.3035 N_Shore	cg18656763
6	3849272		FAM50B	4.43E-10	-0.6610	-1.0304	-0.3694 Island	cg01570885
6	3849277		FAM50B	1.89E-09	-0.4439	-0.8145	-0.3705 Island	cg09821214
6	3849327		FAM50B	3.66E-08	-0.8360	-0.9379	-0.1019 Island	cg25195497
6	3849331		FAM50B	5.39E-11	-0.9456	-1.0647	-0.1191 Island	cg21740964
6	3849381		FAM50B	4.75E-14	-0.8981	-0.9877	-0.0896 Island	cg12840312
6	3849391		FAM50B	3.86E-10	-0.7081	-1.0549	-0.3468 Island	cg01905633
6	3849411		FAM50B	3.93E-14	-0.9157	-1.4247	-0.5091 Island	cg21177626
6	3849434		FAM50B	5.74E-13	-0.7280	-0.7048	0.0232 Island	cg03954573
6	3849458		FAM50B	7.79E-15	-1.0351	-0.9547	0.0804 Island	cg18197332
6	3849475		FAM50B	3.39E-15	-1.0198	-0.9807	0.0391 Island	cg04447621
6	3849536		FAM50B	5.74E-12	-0.8090	-0.8319	-0.0229 Island	cg23835083
6	3849542		FAM50B	1.36E-12	-0.9638	-0.9660	-0.0022 Island	cg18487516
6	3849577		FAM50B	6.94E-14	-1.2180	-0.8288	0.3891 Island	cg12497786
6	3849702		FAM50B;FAM50B	2.52E-15	-0.6510	-0.9402	-0.2892 Island	cg25073793
6	3849801		FAM50B	1.12E-11	-0.5342	-0.5221	0.0121 Island	cg27445347
6	3849818		FAM50B	3.16E-12	-0.5764	-0.6148	-0.0385 Island	cg13101072
15	99408636	870	5 IGF1R	1.05E-11	-1.0990	-0.3361	0.7629 NA	cg19322380
15	99408804		IGF1R	2.68E-12	-0.8773	-0.8485	0.0288 NA	cg21746425
15	99409194		IGF1R	8.53E-12	-0.7750	-0.8589	-0.0840 NA	cg07615383
15	99409411		IGF1R	2.39E-10	-0.8116	-0.6407	0.1709 NA	cg13812291
15	99409506		IGF1R	1.62E-08	-0.7458	-0.7297	0.0161 NA	cg03380198
19	54040774	17311	11 ZNF331;ZNF331	2.25E-36	-1.4733	-1.7058	-0.2325 N_Shore	cg20646939
19	54040813		ZNF331;ZNF331	9.04E-36	-1.3047	-1.3603	-0.0556 Island	cg06855497
19	54041163		ZNF331;ZNF331	1.08E-20	-1.2049	-2.0075	-0.8026 Island	cg22475353
19	54041251		ZNF331;ZNF331	4.62E-25	-1.1806	-1.9457	-0.7651 Island	cg27296330
19	54041329		ZNF331;ZNF331	1.48E-12	-1.2306	-1.8085	-0.5779 Island	cg04522821
19	54041398		ZNF331;ZNF331;ZNF331	6.35E-08	-1.0715	-1.4794	-0.4079 Island	cg05338009
19	54041856		ZNF331;ZNF331	3.87E-31	-1.3937	-1.8075	-0.4138 Island	cg03499639
19	54057208		ZNF331;ZNF331;ZNF331	3.48E-30	-1.1343	-1.2040	-0.0698 N_Shore	cg06860848
19	54057415		ZNF331;ZNF331;ZNF331	1.85E-15	-1.3333	-1.0487	0.2846 Island	cg03113572
19	54057705		ZNF331;ZNF331;ZNF331	5.52E-20	-1.3016	-2.0164	-0.7148 Island	cg19696891
19	54058085		ZNF331;ZNF331;ZNF331	1.37E-27	-1.2247	-1.3533	-0.1286 Island	cg20071427
20	30134929	433	9 HM13;HM13;HM13;P5	6.80E-15	-0.7046	-0.8990	-0.1944 N_Shore	cg25359645
20	30134973		HM13;HM13;HM13;P5	3.32E-22	-0.7675	-0.5430	0.2244 N_Shore	cg24607140
20	30135108		HM13;HM13;HM13;P5	5.36E-15	-0.7530	-0.7201	0.0329 Island	cg06000530
20	30135124		HM13;HM13;HM13;P5	1.24E-17	-0.8512	-0.8225	0.0287 Island	cg19617948
20	30135144		HM13;HM13;HM13;P5	8.25E-17	-0.7793	-0.8702	-0.0909 Island	cg15815607
20	30135149		HM13;HM13;HM13;P5	4.63E-15	-0.7266	-1.0459	-0.3193 Island	cg25645178
20	30135158		HM13;HM13;HM13;P5	4.65E-11	-0.5558	-1.0966	-0.5408 Island	cg17840843
20	30135291		HM13;HM13;HM13;P5	1.44E-11	-0.6070	-0.9686	-0.3616 Island	cg14175568
20	30135362		HM13;HM13;HM13;P5	1.30E-17	-0.6927	-1.0868	-0.3941 S_Shore	cg20129782
20	36148928	524	4 BLCAP;BLCAP;BLCAP;B	9.90E-09	-0.8162	-0.0845	0.7317 Island	cg22943498
20	36149081		BLCAP;BLCAP;BLCAP;B	7.50E-09	-0.6844	-0.1175	0.5669 Island	cg24675557
20	36149231		BLCAP;BLCAP;BLCAP;B	1.43E-09	-0.6123	-0.5525	0.0598 Island	cg16648571
20	36149452		BLCAP;NNAT;BLCAP;BI	1.84E-08	-0.5190	-0.2504	0.2685 Island	cg25962605
20	42142417	1085	13 L3MBTL;L3MBTL	1.03E-08	-0.3862	-0.6922	-0.3060 N_Shore	cg22457903
20	42142484		L3MBTL;L3MBTL	3.52E-11	-0.4638	-0.5796	-0.1158 N_Shore	cg17091610
20	42142494		L3MBTL;L3MBTL	2.31E-14	-0.5965	-0.6442	-0.0477 N_Shore	cg23626798
20	42142559		L3MBTL;L3MBTL	2.42E-13	-0.7693	-0.6026	0.1667 N_Shore	cg15388309
20	42142751		L3MBTL;L3MBTL	2.15E-13	-0.8735	-0.7345	0.1390 N_Shore	cg20529070
20	42142766		L3MBTL;L3MBTL	2.50E-13	-0.8657	-0.7416	0.1241 N_Shore	cg10360552
20	42142847		L3MBTL;L3MBTL	3.36E-12	-1.0066	-1.2731	-0.2665 N_Shore	cg01877937
20	42142852		L3MBTL;L3MBTL	2.26E-12	-0.9933	-1.1082	-0.1149 N_Shore	cg08633313
20	42142897		L3MBTL;L3MBTL	4.18E-08	-0.7472	-1.0554	-0.3082 N_Shore	cg12699433
20	42143080		L3MBTL;L3MBTL;L3ME	1.65E-11	-0.8396	-0.5679	0.2717 N_Shore	cg01071811
20	42143211		L3MBTL;L3MBTL	3.02E-14	-0.8724	-0.7562	0.1162 Island	cg20252111
20	42143399		L3MBTL;L3MBTL	7.40E-13	-0.9704	-0.3655	0.6050 Island	cg15302378
20	42143502		L3MBTL;L3MBTL	2.51E-13	-1.0324	-0.9072	0.1251 Island	cg02472486
Non-ID 80 probes 7 loci								
6	144328421	1408	14 HYMAI;PLAGL1;PLAGL	2.01E-35	-1.2390	-0.2435	0.9955 N_Shore	cg09730369
6	144328482		HYMAI;PLAGL1;PLAGL	3.00E-36	-1.2105	-0.8460	0.3645 N_Shore	cg17865602
6	144328917		HYMAI;PLAGL1;PLAGL	4.39E-51	-1.3955	-1.7077	-0.3122 Island	cg25350411
6	144329052		HYMAI;PLAGL1;PLAGL	1.64E-33	-1.1309	-0.9811	0.1498 Island	cg07077459
6	144329172		HYMAI;PLAGL1;PLAGL	1.71E-21	-0.8325	-0.6717	0.1608 Island	cg22378065
6	144329331		PLAGL1;HYMAI;PLAGL	3.79E-10	-0.4509	-0.4948	-0.0438 Island	cg10007452
6	144329382		PLAGL1;HYMAI;PLAGL	7.49E-20	-0.7417	-0.4879	0.2538 Island	cg22352234
6	144329473		PLAGL1;HYMAI;PLAGL	7.77E-30	-1.0557	-0.6396	0.4160 Island	cg00702231
6	144329485		PLAGL1;HYMAI;PLAGL	8.61E-22	-0.8155	-0.9241	-0.1086 Island	cg12757684

6	144329780			HYMAI;PLAGL1;PLAGL	5.14E-25	-0.9826	-0.8828	0.0998	Island	cg08263357
6	144329789			HYMAI;PLAGL1;PLAGL	2.69E-28	-1.1100	-1.0010	0.1090	Island	cg11532302
6	144329829			HYMAI;PLAGL1;PLAGL	2.82E-45	-1.0069	-1.1050	-0.0981	Island	cg17895149
6	144329887			PLAGL1;PLAGL1;PLAGL	2.73E-09	-0.5565	-0.2143	0.3423	S_Shore	cg23460430
6	144329909			PLAGL1;PLAGL1;PLAGL	2.26E-27	-1.0120	-0.9570	0.0550	S_Shore	cg14161241
7	130130187	2923	42	MESTIT1;MEST;MEST	3.51E-08	-0.7487	-0.3504	0.3983	N_Shore	cg10767216
7	130130478			MESTIT1;MEST;MEST;I	3.76E-15	-0.5349	-0.6048	-0.0699	N_Shore	cg20826277
7	130130481			MESTIT1;MEST;MEST;I	7.73E-10	-0.5668	-0.5970	-0.0302	N_Shore	cg14584935
7	130130596			MESTIT1;MEST;MEST;I	1.32E-35	-0.7714	-0.9762	-0.2048	N_Shore	cg07427065
7	130130740			MESTIT1;MEST;MEST;I	3.30E-33	-1.2085	-0.8069	0.4015	Island	cg02501418
7	130130747			MESTIT1;MEST;MEST;I	8.76E-23	-1.2623	-0.7234	0.5389	Island	cg08229366
7	130130753			MESTIT1;MEST;MEST;I	1.30E-32	-1.3988	-1.1333	0.2656	Island	cg07224147
7	130130995			MESTIT1;MEST;MEST;I	3.76E-32	-1.1227	-1.6285	-0.5058	Island	cg09003373
7	130131085			MESTIT1;MEST;MEST;I	1.37E-29	-0.8619	-1.3430	-0.4811	Island	cg14088957
7	130131136			MESTIT1;MEST;MEST;I	4.91E-30	-0.8354	-1.1183	-0.2829	Island	cg06100421
7	130131138			MESTIT1;MEST;MEST;I	3.28E-28	-0.8753	-1.2413	-0.3660	Island	cg20297423
7	130131258			MEST;MEST;MEST;ME	6.69E-27	-0.8421	-0.8178	0.0243	Island	cg13917504
7	130131359			MEST;MEST;MEST;ME	1.13E-37	-1.2648	-1.4583	-0.1935	Island	cg21667116
7	130131367			MEST;MEST;MEST;ME	1.34E-31	-1.0647	-1.4326	-0.3679	Island	cg23156962
7	130131403			MEST;MEST;MEST;ME	2.61E-30	-1.1991	-1.0643	0.1348	Island	cg04678950
7	130131480			MEST;MEST;MEST;ME	4.97E-22	-0.8389	-0.3809	0.4580	Island	cg17079325
7	130131484			MEST;MEST;MEST;ME	8.19E-23	-0.8933	-0.2929	0.6004	Island	cg04344875
7	130131566			MEST;MEST;MEST;ME	1.17E-25	-1.3091	-1.3167	-0.0077	Island	cg18934293
7	130131633			MEST;MEST;MEST;ME	1.28E-30	-1.1773	-0.7680	0.4093	Island	cg00286878
7	130131676			MEST;MEST;MEST;ME	8.84E-24	-1.4184	-1.4038	0.0146	Island	cg12347392
7	130131691			MEST;MEST;MEST;ME	3.41E-27	-1.4706	-1.1878	0.2828	Island	cg04786207
7	130131730			MEST;MEST;MEST;ME	1.96E-30	-1.0879	-1.0560	0.0319	Island	cg26708559
7	130131797			MEST;MEST;MEST;ME	3.26E-32	-1.3124	-1.0915	0.2209	Island	cg22705386
7	130131826			MEST;MEST;MEST;ME	3.50E-30	-1.2659	-0.9336	0.3323	Island	cg06212135
7	130131829			MEST;MEST;MEST;ME	1.09E-29	-1.3996	-0.8868	0.5128	Island	cg10249538
7	130131869			MEST;MEST;MEST;ME	2.38E-27	-1.3603	-0.8628	0.4974	Island	cg16823958
7	130131885			MEST;MEST;MEST;ME	5.21E-22	-0.9547	-0.5967	0.3580	Island	cg27338480
7	130131887			MEST;MEST;MEST;ME	5.27E-24	-1.0501	-0.4869	0.5632	Island	cg09080913
7	130131905			MEST;MEST;MEST;ME	1.85E-23	-1.2545	-0.7456	0.5088	Island	cg13104298
7	130131923			MEST;MEST;MEST;ME	2.92E-17	-0.7451	-0.7545	-0.0094	Island	cg20050761
7	130131931			MEST;MEST;MEST;ME	1.48E-16	-0.7031	-0.5838	0.1192	Island	cg07870293
7	130132161			MEST;MEST;MEST;ME	3.78E-19	-0.8627	-0.7039	0.1588	Island	cg05556276
7	130132199			MEST;MEST;MESTIT1;I	7.19E-26	-1.3466	-1.1672	0.1793	Island	cg17580798
7	130132298			MEST;MEST;MESTIT1;I	1.30E-19	-0.8383	-0.6928	0.1455	Island	cg19344806
7	130132319			MEST;MEST;MESTIT1;I	2.38E-23	-0.8826	-0.5043	0.3783	Island	cg21200654
7	130132360			MEST;MEST;MESTIT1;I	9.73E-22	-0.9483	-0.4838	0.4645	Island	cg25519926
7	130132413			MEST;MEST;MESTIT1;I	5.31E-09	-0.8138	-1.8046	-0.9908	Island	cg09462536
7	130132419			MEST;MEST;MESTIT1;I	4.17E-14	-0.8055	-1.4632	-0.6576	Island	cg22592140
7	130132422			MEST;MEST;MESTIT1;I	1.75E-30	-0.9796	-0.6197	0.3599	Island	cg03588221
7	130132727			MEST;MEST;MEST	3.24E-08	-0.6052	-0.6429	-0.0376	Island	cg23312013
7	130132790			MEST;MEST;MEST	4.51E-14	-0.8427	-0.0871	0.7556	Island	cg14952237
7	130133110			MEST;MEST;MEST	2.80E-22	-0.8194	-0.1748	0.6445	Island	cg05260959
11	2715837	6421	26	KCNQ1;KCNQ1OT1;KC	2.55E-10	-0.5258	0.1081	0.6339	NA	cg25204743
11	2720229			KCNQ1;KCNQ1OT1;KC	4.10E-54	-1.8594	-1.5273	0.3321	N_Shore	cg27119222
11	2720463			KCNQ1;KCNQ1OT1;KC	1.57E-54	-1.4367	-1.3310	0.1058	Island	cg00000924
11	2721207			KCNQ1;KCNQ1OT1;KC	3.23E-47	-1.5365	-1.7026	-0.1661	Island	cg14392746
11	2721243			KCNQ1OT1;KCNQ1;KC	9.16E-24	-0.7618	-0.6621	0.0997	Island	cg12077660
11	2721248			KCNQ1OT1;KCNQ1;KC	4.65E-21	-0.9674	-0.7672	0.2003	Island	cg03401726
11	2721351			KCNQ1OT1;KCNQ1;KC	3.03E-21	-0.7902	-0.7151	0.0751	Island	cg08359167
11	2721383			KCNQ1OT1;KCNQ1;KC	1.04E-41	-1.6836	-1.4615	0.2221	Island	cg26104781
11	2721409			KCNQ1OT1;KCNQ1;KC	5.21E-16	-1.3144	-1.3324	-0.0180	Island	cg02219360
11	2721428			KCNQ1OT1;KCNQ1;KC	1.86E-35	-1.3699	-1.3133	0.0566	Island	cg20699737
11	2721437			KCNQ1OT1;KCNQ1;KC	6.56E-31	-1.0121	-1.0307	-0.0186	Island	cg26547719
11	2721480			KCNQ1OT1;KCNQ1;KC	7.59E-40	-1.2828	-1.7440	-0.4612	Island	cg07595203
11	2721610			KCNQ1OT1;KCNQ1;KC	5.86E-35	-0.8783	-1.2689	-0.3906	Island	cg14958441
11	2721619			KCNQ1OT1;KCNQ1;KC	9.88E-25	-0.7871	-0.7178	0.0693	Island	cg27323091
11	2721632			KCNQ1OT1;KCNQ1;KC	2.26E-32	-1.2544	-0.6877	0.5667	Island	cg01873334
11	2721817			KCNQ1OT1;KCNQ1;KC	2.92E-47	-1.3920	-1.0159	0.3761	Island	cg14243741
11	2721866			KCNQ1OT1;KCNQ1;KC	5.56E-52	-1.3594	-1.1906	0.1688	Island	cg05740879
11	2721952			KCNQ1OT1;KCNQ1;KC	1.35E-48	-1.1888	-1.5586	-0.3698	Island	cg01893176
11	2721961			KCNQ1OT1;KCNQ1;KC	9.34E-33	-0.9953	-0.7287	0.2666	Island	cg11993252
11	2722073			KCNQ1OT1;KCNQ1;KC	3.44E-47	-1.3526	-1.6149	-0.2623	Island	cg26094482
11	2722076			KCNQ1OT1;KCNQ1;KC	1.43E-52	-1.7535	-1.9951	-0.2416	Island	cg26908876
11	2722082			KCNQ1OT1;KCNQ1;KC	5.15E-57	-1.7308	-1.5275	0.2033	Island	cg03422070
11	2722084			KCNQ1OT1;KCNQ1;KC	2.75E-55	-1.6435	-1.7278	-0.0843	Island	cg15651941
11	2722119			KCNQ1OT1;KCNQ1;KC	4.27E-68	-1.5133	-1.6154	-0.1021	S_Shore	cg06288089
11	2722195			KCNQ1OT1;KCNQ1;KC	1.33E-47	-1.1939	-1.2913	-0.0975	S_Shore	cg02798157
11	2722258			KCNQ1OT1;KCNQ1;KC	6.15E-50	-1.3412	-0.9271	0.4141	S_Shore	cg27604721
20	57426835	721	4	GNAS;GNAS;GNAS;GN	2.59E-08	-0.3700	-0.3691	0.0009	Island	cg04457481
20	57427210			GNAS;GNAS;GNAS;GN	3.15E-08	-0.4364	-0.4146	0.0218	N_Shore	cg26496204
20	57427472			GNAS;GNAS;GNAS	9.65E-09	-0.9384	-1.5071	-0.5687	N_Shore	cg07105596
20	57427556			GNAS;GNAS;GNAS	1.89E-08	-0.7591	-0.9167	-0.1575	N_Shore	cg14564778

ID impr 86 probes 4 loci

Supplementary Table 5: **TND-HIL candidate hypomethylated loci**- p-value of $> 1.33 \times 10^{-7}$ (0.05 divided by the number of statistical tests), M value between +1 and -1 (equivalent to a beta value of 0.3-0.7) filters were applied. CpG spacing less than 12nt per two CpGs (ie probably in-cis) and >2000 between adjacent CpGs on average (ie probably coincidental) were eliminated.

This gives: 11 new loci with 44 probes,
5 published loci with 71 probes,
5 clinical loci with 74 probes

CHR	MAPINFO	extent of locus	Probe number	UCSC gene name	Adjust Pval	M-Difference	Mean HIL M-value	Mean control M-value	Relation to UCSC CpG island	Probe ID
	1	40024971	261	2 LOC728448	9.52E-19	-1.2411	-0.6974	0.5437	NA	cg10243676
	1	40025232		LOC728448	5.23E-10	-0.9625	-0.5190	0.4435	NA	cg11704876
	4	6107021	318	4 JAKMIP1;JAKMIP1	1.38E-12	-1.0901	-0.4752	0.6149	N_Shore	cg18994250
	4	6107280		JAKMIP1;JAKMIP1	3.46E-32	-1.4522	-1.2868	0.1654	Island	cg23166781
	4	6107320		JAKMIP1;JAKMIP1	1.83E-16	-0.8417	-0.8993	-0.0575	Island	cg06231140
	4	6107339		JAKMIP1;JAKMIP1	1.15E-19	-1.1452	-0.7875	0.3577	Island	cg22098660
	6	170055155	177	2 WDR27	3.34E-22	-3.1348	-2.2049	0.9299	NA	cg11938672
	6	170055332		WDR27	3.56E-09	-2.5930	-2.0510	0.5421	N_Shelf	cg18322025
	7	23529999	690	2 RPS2P32	9.81E-28	-2.4651	-2.9165	-0.4514	N_Shore	cg12829142
	7	23530689		RPS2P32	2.03E-32	-0.8504	-0.7994	0.0510	Island	cg26074723
	7	138348774	669	3 SVOPL;SVOPL	2.34E-14	-1.3107	-1.1937	0.1170	N_Shore	cg05719902
	7	138349158		SVOPL;SVOPL	5.73E-13	-1.8612	-1.0985	0.7628	Island	cg10184328
	7	138349443		SVOPL;SVOPL	1.90E-16	-2.3510	-1.8767	0.4742	Island	cg23085143
	8	37605359	619	6 LOC728024;ERLIN2	3.04E-17	-0.9308	-0.3969	0.5338	NA	cg11496432
	8	37605517		LOC728024;ERLIN2	1.90E-18	-1.6678	-1.9442	-0.2764	NA	cg13346869
	8	37605552		LOC728024;ERLIN2	3.31E-24	-1.5660	-1.8350	-0.2690	NA	cg05020125
	8	37605717		LOC728024;ERLIN2	2.27E-32	-2.0140	-1.6997	0.3142	NA	cg21505509
	8	37605783		LOC728024;ERLIN2	2.67E-38	-2.3179	-2.0549	0.2630	NA	cg08247852
	8	37605978		LOC728024;ERLIN2	4.85E-15	-1.1002	-0.4515	0.6487	NA	cg00450319
	9	98075481	11	2 FANCC	3.82E-41	-1.9796	-1.8573	0.1223	Island	cg14127626
	9	98075492		FANCC	1.26E-50	-1.9978	-1.9070	0.0907	Island	cg21891967
	17	9729250	172	4 GLP2R	8.69E-13	-0.6680	-0.2895	0.3786	NA	cg07669517
	17	9729253		GLP2R	6.27E-20	-0.6057	0.3736	0.9793	NA	cg25656836
	17	9729337		GLP2R	2.36E-16	-0.6613	-0.1958	0.4655	NA	cg22885891
	17	9729422		GLP2R	3.25E-10	-0.8390	-0.2061	0.6329	NA	cg14783904
	18	77905298	649	9 LOC100130522;LOC:	3.28E-18	-2.7370	-3.1539	-0.4169	Island	cg13704680
	18	77905355		LOC100130522;LOC:	1.60E-55	-2.8727	-3.3706	-0.4978	Island	cg16737533
	18	77905408		LOC100130522;LOC:	5.05E-27	-2.6499	-3.4337	-0.7838	Island	cg19774868
	18	77905565		LOC100130522;LOC:	2.48E-42	-2.3277	-2.7460	-0.4183	Island	cg16244155
	18	77905663		LOC100130522;LOC:	5.58E-28	-3.0321	-3.7025	-0.6704	S_Shore	cg20191338
	18	77905699		LOC100130522;LOC:	1.74E-18	-2.7773	-3.6720	-0.8947	S_Shore	cg06092953
	18	77905747		LOC100130522;LOC:	2.79E-17	-2.1445	-2.7239	-0.5794	S_Shore	cg12061113
	18	77905751		LOC100130522;LOC:	9.51E-25	-2.7643	-2.8662	-0.1020	S_Shore	cg13287964
	18	77905947		LOC100130522;LOC:	1.24E-66	-2.5147	-2.8991	-0.3844	S_Shore	cg18687533
	21	40757691	517	4 WRB	8.73E-14	-0.9402	-0.3569	0.5833	Island	cg00606841
	21	40757750		WRB	4.48E-08	-0.8722	-0.5303	0.3420	Island	cg22858667
	21	40757899		WRB	2.75E-25	-1.1913	-0.8116	0.3797	Island	cg26710963
	21	40758208		WRB;WRB	1.44E-22	-0.9087	-1.3811	-0.4724	S_Shore	cg09916765
	22	42078217	506	6 NHP2L1;NHP2L1	7.03E-50	-2.2973	-2.3214	-0.0241	Island	cg18152773
	22	42078330		NHP2L1;NHP2L1	9.89E-47	-2.1277	-1.9036	0.2241	Island	cg05871614
	22	42078365		NHP2L1;NHP2L1;NH	3.36E-48	-2.3207	-2.2536	0.0671	Island	cg22083753
	22	42078388		NHP2L1;NHP2L1;NH	1.74E-44	-1.7714	-1.7219	0.0494	Island	cg15284719
	22	42078567		NHP2L1;NHP2L1	7.89E-48	-2.6382	-2.7232	-0.0850	S_Shore	cg08686092
	22	42078723		NHP2L1;NHP2L1	4.37E-23	-1.3300	-1.3374	-0.0073	S_Shore	cg11536612
Novel	44 probes	11 loci								
	1	68512539	4734	20 DIRAS3	1.15E-20	-1.1183	-1.6316	-0.5132	N_Shore	cg03641225
	1	68512650		DIRAS3	1.13E-11	-1.1729	-0.1989	0.9741	Island	cg24871743
	1	68512777		DIRAS3	1.12E-26	-1.4570	-1.1713	0.2857	Island	cg22901840
	1	68512807		DIRAS3	1.35E-17	-1.2738	-0.4842	0.7896	Island	cg20149168
	1	68512971		DIRAS3	5.30E-18	-1.2788	-0.9535	0.3253	Island	cg09118625
	1	68513063		DIRAS3	1.95E-29	-1.0837	-1.0761	0.0077	S_Shore	cg21808053
	1	68515788		DIRAS3	1.82E-36	-1.0294	-0.0891	0.9403	N_Shore	cg02317907
	1	68515977		DIRAS3	1.93E-26	-0.8299	-0.2684	0.5615	N_Shore	cg19114595
	1	68516080		DIRAS3	8.60E-57	-1.4230	-1.3754	0.0475	N_Shore	cg12070746
	1	68516138		DIRAS3	1.93E-49	-1.6927	-1.6846	0.0081	N_Shore	cg25755905
	1	68516272		DIRAS3;DIRAS3	1.44E-59	-1.5850	-1.1513	0.4336	Island	cg22500004
	1	68516374		DIRAS3;DIRAS3	4.35E-28	-1.3423	-1.3942	-0.0519	Island	cg19694923
	1	68516453		DIRAS3;DIRAS3	3.39E-57	-1.5734	-1.3064	0.2670	Island	cg05392265
	1	68516463		DIRAS3	4.23E-56	-1.7130	-1.3052	0.4078	Island	cg06191076
	1	68516465		DIRAS3	5.42E-59	-2.0618	-1.2930	0.7688	Island	cg16148270
	1	68516518		DIRAS3	8.36E-50	-1.6703	-1.5116	0.1586	N_Shore	cg13208159
	1	68517177		DIRAS3	3.36E-24	-1.1609	-1.0860	0.0749	N_Shore	cg27545611
	1	68517205		DIRAS3	2.98E-37	-1.5705	-1.6182	-0.0477	N_Shore	cg16148134
	1	68517255		DIRAS3	4.05E-54	-1.4129	-1.2177	0.1952	Island	cg13605615
	1	68517273		DIRAS3	1.28E-41	-1.6666	-1.3981	0.2685	Island	cg10038185

6	3849272	546	17	FAM50B	1.13E-11	-0.6122	-0.5868	0.0254	Island	cg01570885
6	3849277			FAM50B	8.75E-09	-0.4044	-0.3121	0.0923	Island	cg09821214
6	3849327			FAM50B	5.28E-09	-0.7997	-0.3678	0.4319	Island	cg25195497
6	3849331			FAM50B	3.24E-13	-0.8576	-0.5002	0.3574	Island	cg21740964
6	3849381			FAM50B	1.43E-13	-0.7578	-0.8212	-0.0634	Island	cg12840312
6	3849391			FAM50B	5.03E-11	-0.8045	-1.0637	-0.2592	Island	cg01905633
6	3849411			FAM50B	9.76E-10	-0.7851	-1.2130	-0.4279	Island	cg21177626
6	3849434			FAM50B	4.01E-18	-0.8746	-0.3854	0.4893	Island	cg03954573
6	3849458			FAM50B	1.35E-18	-1.0194	-0.9167	0.1027	Island	cg18197332
6	3849475			FAM50B	1.07E-23	-1.1455	-1.1062	0.0392	Island	cg04447621
6	3849536			FAM50B	9.54E-32	-1.3015	-0.9342	0.3673	Island	cg23835083
6	3849542			FAM50B	2.31E-31	-1.4204	-0.9688	0.4516	Island	cg18487516
6	3849577			FAM50B	1.33E-35	-1.6247	-1.2336	0.3911	Island	cg12497786
6	3849690			FAM50B;FAM50B	5.79E-11	-0.8169	-0.8202	-0.0033	Island	cg21153160
6	3849702			FAM50B;FAM50B	4.40E-24	-0.7593	-0.6873	0.0720	Island	cg25073793
6	3849801			FAM50B	6.56E-10	-0.4698	-0.0789	0.3909	Island	cg27445347
6	3849818			FAM50B	2.23E-08	-0.4983	-0.2410	0.2573	Island	cg13101072
15	99408636	1321	6	IGF1R	1.09E-31	-1.7231	-0.7473	0.9758	NA	cg19322380
15	99408804			IGF1R	1.78E-19	-1.1573	-1.1205	0.0368	NA	cg21746425
15	99409194			IGF1R	1.34E-18	-1.1053	-1.3848	-0.2796	NA	cg07615383
15	99409360			IGF1R	2.08E-20	-1.4138	-1.4788	-0.0651	NA	cg00098799
15	99409506			IGF1R	7.22E-33	-1.4966	-1.2694	0.2273	NA	cg03380198
15	99409957			IGF1R	4.39E-13	-0.7410	-0.0528	0.6881	NA	cg11544420
19	54040813	17272	10	ZNF331;ZNF331	1.34E-48	-1.9680	-1.6224	0.3456	Island	cg06855497
19	54041163			ZNF331;ZNF331	8.48E-29	-1.9414	-2.6707	-0.7292	Island	cg22475353
19	54041251			ZNF331;ZNF331	2.07E-28	-1.7684	-2.3009	-0.5325	Island	cg27296330
19	54041329			ZNF331;ZNF331	1.19E-14	-1.8432	-2.0353	-0.1921	Island	cg04522821
19	54041856			ZNF331;ZNF331	8.20E-34	-2.0526	-2.0620	-0.0093	Island	cg03499639
19	54041999			ZNF331;ZNF331	1.32E-07	-0.4954	-0.4601	0.0353	S_Shore	cg25409185
19	54057208			ZNF331;ZNF331;ZNF	4.52E-40	-1.7364	-1.4420	0.2945	N_Shore	cg06860848
19	54057415			ZNF331;ZNF331;ZNF	1.28E-37	-2.0271	-1.3890	0.6380	Island	cg03113572
19	54057705			ZNF331;ZNF331;ZNF	5.33E-22	-1.6699	-2.0806	-0.4107	Island	cg19696891
19	54058085			ZNF331;ZNF331;ZNF	3.82E-24	-1.7000	-1.4042	0.2958	Island	cg20071427
20	42142417	1072	18	L3MBTL;L3MBTL	1.76E-12	-0.5068	-0.3185	0.1883	N_Shore	cg22457903
20	42142451			L3MBTL;L3MBTL	2.72E-21	-0.8238	-0.3132	0.5106	N_Shore	cg20091959
20	42142484			L3MBTL;L3MBTL	2.49E-13	-0.5947	-0.2569	0.3378	N_Shore	cg17091610
20	42142494			L3MBTL;L3MBTL	1.90E-18	-0.6703	-0.3311	0.3392	N_Shore	cg23626798
20	42142559			L3MBTL;L3MBTL	2.89E-19	-0.9518	-0.4697	0.4821	N_Shore	cg15388309
20	42142596			L3MBTL;L3MBTL	7.67E-09	-0.7536	-0.6161	0.1375	N_Shore	cg16862791
20	42142671			L3MBTL;L3MBTL	8.01E-17	-0.9994	-0.6103	0.3891	N_Shore	cg06446163
20	42142673			L3MBTL;L3MBTL	2.86E-08	-0.8229	-0.6119	0.2110	N_Shore	cg04984575
20	42142751			L3MBTL;L3MBTL	2.40E-16	-1.0002	-0.4821	0.5181	N_Shore	cg20529070
20	42142766			L3MBTL;L3MBTL	6.20E-10	-0.7242	-0.6366	0.0876	N_Shore	cg10360552
20	42142847			L3MBTL;L3MBTL	4.22E-14	-1.2682	-1.1909	0.0772	N_Shore	cg01877937
20	42142852			L3MBTL;L3MBTL	1.98E-09	-0.9780	-0.7737	0.2043	N_Shore	cg08633313
20	42142897			L3MBTL;L3MBTL	2.24E-10	-0.9061	-0.8109	0.0951	N_Shore	cg12699433
20	42142947			L3MBTL;L3MBTL	7.87E-08	-0.8141	-0.6338	0.1803	N_Shore	cg11319028
20	42143174			L3MBTL;L3MBTL;L3M	9.62E-14	-1.1475	-0.6252	0.5223	N_Shore	cg15330298
20	42143211			L3MBTL;L3MBTL	1.45E-09	-0.6936	-0.4937	0.1998	Island	cg20252111
20	42143399			L3MBTL;L3MBTL	5.23E-08	-0.7687	-0.1637	0.6050	Island	cg15302378
20	42143489			L3MBTL;L3MBTL	5.54E-09	-0.9348	-0.3812	0.5537	Island	cg09541000

non-ID imprinted 71 probes 5 loci

6	144328482	1427	15	HYMAI;PLAGL1;PLAC	4.84E-124	-2.9854	-2.3038	0.6817	N_Shore	cg17865602
6	144328917			HYMAI;PLAGL1;PLAC	7.26E-105	-3.5554	-3.4813	0.0741	Island	cg25350411
6	144329052			HYMAI;PLAGL1;PLAC	4.95E-111	-4.0695	-3.7324	0.3371	Island	cg07077459
6	144329172			HYMAI;PLAGL1;PLAC	1.23E-106	-3.9540	-3.6328	0.3212	Island	cg22378065
6	144329331			PLAGL1;HYMAI;PLAC	2.90E-88	-3.3349	-3.2891	0.0459	Island	cg10007452
6	144329473			PLAGL1;HYMAI;PLAC	5.39E-103	-3.8291	-3.2703	0.5587	Island	cg00702231
6	144329485			PLAGL1;HYMAI;PLAC	3.39E-97	-3.2522	-3.2307	0.0215	Island	cg12757684
6	144329732			HYMAI;PLAGL1;PLAC	1.88E-19	-1.7927	-1.5657	0.2270	Island	cg21952820
6	144329766			HYMAI;PLAGL1;PLAC	2.95E-94	-3.1572	-3.0922	0.0650	Island	cg05326984
6	144329780			HYMAI;PLAGL1;PLAC	5.70E-106	-3.6264	-3.0149	0.6115	Island	cg08263357
6	144329789			HYMAI;PLAGL1;PLAC	2.77E-79	-2.7299	-2.5953	0.1345	Island	cg11532302
6	144329802			HYMAI;PLAGL1;PLAC	4.74E-70	-2.0691	-2.1695	-0.1005	Island	cg27216384
6	144329829			HYMAI;PLAGL1;PLAC	1.82E-114	-3.0906	-2.7493	0.3413	Island	cg17895149
6	144329887			PLAGL1;PLAGL1;PLA	2.05E-24	-0.9802	-0.2299	0.7503	S_Shore	cg23460430
6	144329909			PLAGL1;PLAGL1;PLA	2.25E-58	-1.7004	-1.3800	0.3204	S_Shore	cg14161241
7	94286208	461	6	SGCE;PEG10;SGCE;P	2.61E-09	-0.5134	-0.0137	0.4996	Island	cg16492735
7	94286219			SGCE;PEG10;SGCE;P	4.84E-08	-0.4458	-0.1058	0.3400	Island	cg09512080
7	94286243			SGCE;PEG10;SGCE;P	6.45E-10	-0.3908	0.0715	0.4623	Island	cg26503018
7	94286263			SGCE;PEG10;SGCE;P	1.42E-08	-0.3326	0.0751	0.4078	Island	cg21771834
7	94286343			SGCE;PEG10;SGCE;P	4.19E-08	-0.4294	0.0191	0.4486	Island	cg03384175
7	94286669			SGCE;PEG10;SGCE;P	1.28E-09	-0.5122	-0.1387	0.3735	S_Shore	cg20041873
7	130130383	2727	42	MESTIT1;MEST;MES	1.13E-19	-1.1900	-0.6866	0.5035	N_Shore	cg26275543
7	130130478			MESTIT1;MEST;MES	2.08E-09	-0.3814	-0.1981	0.1832	N_Shore	cg20826277
7	130130596			MESTIT1;MEST;MES	4.14E-27	-0.9546	-0.8015	0.1532	N_Shore	cg07427065
7	130130740			MESTIT1;MEST;MES	8.38E-35	-1.8889	-1.2642	0.6247	Island	cg02501418
7	130130747			MESTIT1;MEST;MES	2.27E-29	-1.7699	-1.0116	0.7583	Island	cg08229366

7	130130918		MESTIT1;MEST;MES	2.37E-36	-2.3317	-1.7539	0.5778	Island	cg27417677
7	130130995		MESTIT1;MEST;MES	8.00E-31	-1.7813	-2.0994	-0.3181	Island	cg09003373
7	130131085		MESTIT1;MEST;MES	7.26E-24	-1.2306	-1.5467	-0.3161	Island	cg14088957
7	130131136		MESTIT1;MEST;MES	1.67E-28	-1.4721	-1.4461	0.0260	Island	cg06100421
7	130131138		MESTIT1;MEST;MES	2.28E-26	-1.4594	-1.4946	-0.0352	Island	cg20297423
7	130131146		MESTIT1;MEST;MES	1.57E-25	-1.7840	-1.9463	-0.1623	Island	cg05369791
7	130131258		MEST;MEST;MEST;N	1.96E-38	-1.6033	-1.2068	0.3964	Island	cg13917504
7	130131268		MEST;MEST;MEST;N	5.54E-38	-1.9035	-1.4650	0.4385	Island	cg25407198
7	130131359		MEST;MEST;MEST;N	8.44E-33	-2.0692	-2.0975	-0.0283	Island	cg21667116
7	130131367		MEST;MEST;MEST;N	3.31E-34	-1.7991	-2.0256	-0.2264	Island	cg23156962
7	130131403		MEST;MEST;MEST;N	5.38E-35	-2.3005	-1.9313	0.3692	Island	cg04678950
7	130131480		MEST;MEST;MEST;N	2.69E-40	-2.3025	-1.4946	0.8080	Island	cg17079325
7	130131633		MEST;MEST;MEST;N	3.77E-38	-2.1088	-1.4459	0.6628	Island	cg00286878
7	130131676		MEST;MEST;MEST;N	9.20E-29	-2.1620	-1.8605	0.3015	Island	cg12347392
7	130131691		MEST;MEST;MEST;N	1.14E-29	-2.1769	-1.5815	0.5954	Island	cg04786207
7	130131730		MEST;MEST;MEST;N	2.61E-37	-2.1744	-1.7182	0.4561	Island	cg26708559
7	130131797		MEST;MEST;MEST;N	8.44E-33	-2.3238	-1.8190	0.5049	Island	cg22705386
7	130131826		MEST;MEST;MEST;N	1.51E-31	-2.0754	-1.3725	0.7028	Island	cg06212135
7	130131829		MEST;MEST;MEST;N	1.76E-25	-1.9267	-1.4901	0.4366	Island	cg10249538
7	130131869		MEST;MEST;MEST;N	1.54E-32	-2.5171	-1.9711	0.5460	Island	cg16823958
7	130131885		MEST;MEST;MEST;N	1.41E-32	-2.1542	-1.7240	0.4302	Island	cg27338480
7	130131887		MEST;MEST;MEST;N	3.11E-32	-1.9845	-1.3402	0.6443	Island	cg09080913
7	130131905		MEST;MEST;MEST;N	5.61E-34	-2.4316	-1.8341	0.5975	Island	cg13104298
7	130131916		MEST;MEST;MEST;N	1.27E-13	-1.9989	-1.7912	0.2077	Island	cg07315018
7	130131921		MEST;MEST;MEST;N	2.61E-19	-1.9082	-2.0744	-0.1663	Island	cg21629528
7	130131923		MEST;MEST;MEST;N	1.42E-33	-2.3148	-2.2089	0.1059	Island	cg20050761
7	130131931		MEST;MEST;MEST;N	2.69E-32	-1.9811	-1.7874	0.1937	Island	cg07870293
7	130132161		MEST;MEST;MEST;N	4.04E-31	-1.8439	-1.5778	0.2661	Island	cg05556276
7	130132199		MEST;MEST;MESTIT	2.32E-33	-2.2688	-1.9891	0.2797	Island	cg17580798
7	130132265		MEST;MEST;MESTIT	2.38E-29	-2.1985	-2.2797	-0.0811	Island	cg01784351
7	130132319		MEST;MEST;MESTIT	2.34E-40	-1.7264	-0.9787	0.7477	Island	cg21200654
7	130132360		MEST;MEST;MESTIT	8.87E-30	-1.5860	-1.1854	0.4006	Island	cg25519926
7	130132413		MEST;MEST;MESTIT	1.83E-30	-1.6883	-2.2849	-0.5965	Island	cg09462536
7	130132419		MEST;MEST;MESTIT	2.42E-31	-1.8283	-1.9517	-0.1234	Island	cg22592140
7	130132422		MEST;MEST;MESTIT	2.02E-41	-1.9416	-1.3567	0.5849	Island	cg03588221
7	130132727		MEST;MEST;MEST	1.14E-30	-1.2002	-0.9373	0.2629	Island	cg23312013
7	130133110		MEST;MEST;MEST	2.69E-32	-1.2818	-0.6701	0.6117	Island	cg05260959
11	2720463	1656	9 KCNQ1;KCNQ1OT1;KCNQ1	1.03E-08	-0.6924	-0.4016	0.2908	Island	cg00000924
11	2721610		KCNQ1OT1;KCNQ1;KCNQ1	1.26E-07	-0.5269	-0.4296	0.0973	Island	cg14958441
11	2721799		KCNQ1OT1;KCNQ1;KCNQ1	4.17E-09	-0.7227	-0.2090	0.5138	Island	cg05816130
11	2721817		KCNQ1OT1;KCNQ1;KCNQ1	1.22E-07	-0.7204	0.0283	0.7487	Island	cg14243741
11	2721857		KCNQ1OT1;KCNQ1;KCNQ1	9.47E-10	-0.7921	-0.2013	0.5908	Island	cg21137515
11	2721952		KCNQ1OT1;KCNQ1;KCNQ1	3.03E-09	-0.6767	-0.5174	0.1593	Island	cg01893176
11	2722082		KCNQ1OT1;KCNQ1;KCNQ1	2.06E-08	-0.7978	-0.1692	0.6287	Island	cg03422070
11	2722086		KCNQ1OT1;KCNQ1;KCNQ1	3.55E-08	-0.7901	-0.3582	0.4319	Island	cg25306939
11	2722119		KCNQ1OT1;KCNQ1;KCNQ1	1.91E-08	-0.6791	-0.4582	0.2208	S_Shore	cg06288089
15	25068738	31	2 SNRPN;SNRPN;SNRP	1.20E-11	-0.5727	-0.1451	0.4276	NA	cg11265941
15	25068769		SNRPN;SNRPN;SNRP	4.56E-10	-0.4591	0.1647	0.6238	NA	cg27304225

ID imprinted 74 probes 5 loci

Supplementary Table 6: Resolution of DNA methylation at the SNRPN locus in patients with TND-HIL and BWS-HIL. Methylation data are presented for all CpGs passing QC within the SNRPN locus. Statistical criteria for hypomethylation are: control M-value between -1 and +1, beta-difference <0; P-value and adjusted P-value <1e-7. Only at two probes in TND-HIL patients are these inclusion criteria met (highlighted in red). nd: no data (probe failed initial QC).

CHR	MAPINFO	ILMNID	UCSC REFGENE NAME	BWS-HIL					TND-HIL				
				P-Value	Adjusted P-value	Beta-Difference	Mean BWS	Mean control	P-Value	Adjusted P-value	Beta-Difference	Mean TND-HIL	Mean control
15	25068564	cg22491305	SNRPN	0.06	0.26	-0.22	1.54	1.75	0.07	0.39	-0.17	1.81	1.98
15	25068738	cg11265941	SNRPN	0.06	0.27	-0.13	-0.04	0.09	5.6E-15	1.2E-11	-0.57	-0.15	0.43
15	25068754	cg11826663	SNRPN	1.8E-08	3.6E-06	-0.38	-0.05	0.33	1.8E-03	0.06	-0.22	0.15	0.38
15	25068757	cg24785225	SNRPN	nd					2.4E-04	0.02	-0.30	0.17	0.46
15	25068763	cg10271763	SNRPN	1.4E-08	2.9E-06	-0.41	-0.09	0.31	nd				
15	25068769	cg27304225	SNRPN	2.6E-04	0.01	-0.20	0.07	0.27	2.3E-13	4.6E-10	-0.46	0.16	0.62
15	25068790	cg19803984	SNRPN	2.9E-03	0.04	-0.19	-0.36	-0.18	1.3E-07	8.5E-05	-0.38	-0.21	0.16
15	25068850	cg16321029	SNRPN	nd					1.0E-08	9.5E-06	-0.63	-0.59	0.04
15	25069376	cg26033681	SNRPN	0.02	0.16	0.22	0.37	0.15	0.35	0.73	0.09	0.66	0.57
15	25092069	cg25030262	SNRPN	0.01	0.06	-0.36	-0.15	0.22	0.01	0.16	-0.31	0.24	0.54
15	25093244	cg25978208	SNRPN	0.16	0.45	-0.12	-0.32	-0.21	1.6E-03	0.06	-0.30	-0.02	0.28
15	25093366	cg02171545	SNRPN	0.51	0.78	0.12	-0.57	-0.69	0.95	0.99	0.01	-0.49	-0.50
15	25093456	cg02305723	SNRPN	0.01	0.06	-0.36	-0.05	0.31	0.11	0.47	-0.18	-0.40	-0.22
15	25093521	cg22678136	SNRPN	nd					0.97	0.99	0.00	-0.17	-0.17
15	25094139	cg13887424	SNRPN	0.94	0.98	0.01	2.33	2.32	0.34	0.72	-0.07	2.31	2.38
15	25096573	cg19964320	SNRPN	nd					0.88	0.97	-0.01	0.00	0.01
15	25101627	cg01240229	SNRPN	1.7E-05	9.5E-04	-0.32	0.61	0.92	7.2E-07	3.2E-04	-0.30	0.76	1.06
15	25101646	cg27233338	SNRPN	1.4E-03	0.02	-0.29	1.20	1.49	0.49	0.82	-0.05	1.53	1.58
15	25101680	cg10428394	SNRPN	0.45	0.74	-0.08	0.16	0.24	nd				
15	25108042	cg26939721	SNRPN	0.82	0.94	-0.02	-0.84	-0.82	0.01	0.19	-0.18	-0.68	-0.50
15	25119502	cg22259765	SNRPN	0.65	0.86	0.05	-0.61	-0.66	0.46	0.80	0.09	-0.10	-0.19
15	25123287	cg27644292	SNRPN	0.02	0.12	-0.37	-0.12	0.25	0.42	0.78	-0.14	0.45	0.59
15	25123381	cg08560373	SNRPN	nd					0.57	0.86	0.10	-0.65	-0.75
15	25123491	cg25657700	SNRPN	0.01	0.11	-0.24	0.10	0.34	5.6E-04	0.03	-0.34	0.30	0.64
15	25123549	cg24993443	SNRPN	0.42	0.72	-0.14	-0.40	-0.27	0.63	0.88	-0.08	-0.03	0.05
15	25123731	cg21870668	SNRPN	0.45	0.74	-0.09	-0.37	-0.28	0.22	0.62	-0.15	-0.04	0.12
15	25124213	cg21061553	SNRPN	0.86	0.95	-0.03	1.86	1.90	0.98	1.00	0.00	2.19	2.19
15	25145254	cg23075611	SNRPN	0.89	0.96	-0.01	-0.40	-0.39	1.2E-03	0.05	-0.24	-0.26	-0.03
15	25165585	cg09206878	SNRPN	0.62	0.84	0.06	1.52	1.45	1.5E-03	0.06	0.37	2.04	1.67
15	25196084	cg11152012	SNRPN	0.55	0.81	-0.05	0.51	0.56	0.35	0.73	-0.08	0.60	0.67
15	25198793	cg21746532	SNRPN;SNURF	0.06	0.27	0.40	2.45	2.04	0.59	0.86	0.05	2.29	2.24
15	25199028	cg01432432	SNRPN;SNURF	0.27	0.59	-0.14	2.71	2.85	0.65	0.89	0.05	2.90	2.85
15	25199057	cg08372135	SNRPN;SNURF	nd					0.96	0.99	0.00	3.03	3.03
15	25199164	cg03858387	SNRPN;SNURF	0.21	0.52	0.12	1.57	1.45	0.21	0.60	0.12	1.65	1.53
15	25199270	cg02152271	SNRPN;SNURF	nd					0.26	0.66	-0.10	2.24	2.34
15	25200253	cg18506672	SNRPN;SNURF	0.01	0.06	-0.17	-0.30	-0.13	5.0E-05	0.01	-0.41	-0.37	0.04
15	25200406	cg02125271	SNRPN;SNURF	3.8E-06	2.9E-04	-0.31	0.52	0.83	1.6E-06	5.8E-04	-0.42	0.45	0.87
15	25200490	cg26875073	SNRPN;SNURF	nd					0.02	0.23	-0.27	-0.28	0.00
15	25201020	cg22159025	SNRPN;SNURF	1.7E-03	0.03	-0.29	-0.76	-0.47	0.03	0.28	-0.26	-0.50	-0.24
15	25201224	cg22555495	SNRPN;SNURF	1.7E-04	0.01	-0.19	-0.37	-0.18	1.2E-07	7.9E-05	-0.39	-0.06	0.34
15	25201429	cg01614564	SNRPN;SNURF	nd					1.9E-07	1.1E-04	-0.30	0.31	0.61
15	25201732	cg13073261	SNRPN;SNURF	1.4E-05	8.3E-04	-0.32	-0.32	0.00	1.1E-03	0.05	-0.27	-0.27	0.01
15	25203270	cg20775837	SNRPN;SNURF	nd					0.16	0.55	0.15	2.29	2.15
15	25215375	cg14851390	SNRPN;SNURF	nd					0.04	0.32	0.20	2.49	2.29
15	25221513	cg25705379	SNRPN;SNURF	0.32	0.64	0.09	1.93	1.83	0.76	0.93	0.03	2.06	2.03
15	25223574	cg04195863	SNRPN;SNURF	0.31	0.62	0.12	1.84	1.72	0.10	0.46	0.18	2.12	1.94
15	25223633	cg15477139	SNRPN;SNURF	0.07	0.29	-0.29	0.18	0.47	nd				